Colloids and Surfaces A: Physicochemical and Engineering Aspects 691 (2024) 133844

Contents lists available at ScienceDirect

Colloids and Surfaces A: Physicochemical and Engineering Aspects

journal homepage: www.elsevier.com/locate/colsurfa

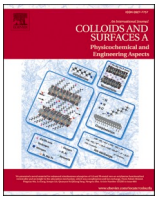

Role of temperature and urea for surface and foam properties of nonionic surfactants with dodecyl alkyl chain

Lucie Delforce, Slavka Tcholakova *

Department of Chemical Engineering, Sofia University, Sofia, Bulgaria

GRAPHICAL ABSTRACT

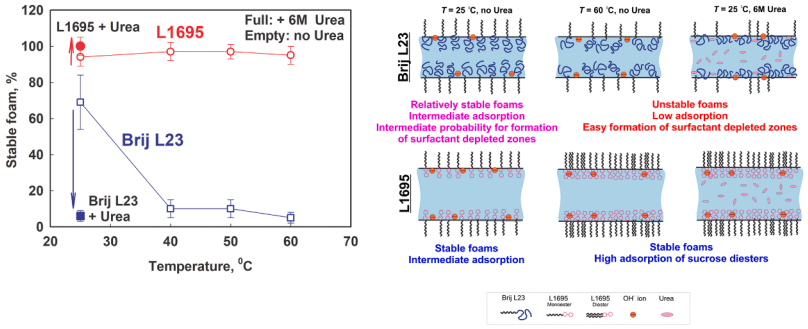

ARTICLE INFO

Keywords:
foam
hydrogen bond
sucrose ester
Brij
surface coverage
Bartsch test
foam rise method
Urea

ABSTRACT

The surface, film and foam properties of two nonionic surfactants, dodecyl sucrose ester (L1695) and dodecyl polyoxyethylene ether (Brij L23), were studied at four different temperatures between 25 and 60 °C and three surfactant concentrations (0.01%, 0.1%, and 1% wt.). The impact of 6 M urea was also assessed to determine the role of hydrogen bonds for the observed trends. The foams were generated using two methods: the fast foaming method (Bartsch test), producing foams with smaller bubbles, and the slow foaming method (foam rise method), yielding foams with bigger bubbles. For Brij L23, an increase in temperature resulted in a decrease in the critical micellar concentration (CMC), reduced surfactant adsorption on the air-water interface, weakened electrostatic repulsion between the foam film surfaces and significantly decreased foam stability. For L1695, an increase in temperature increased surfactant adsorption, maximized the foamability at 40 °C, and did not affect the foam stability for foams with small bubbles. However, the temperature increase leads to decreased stability at low

Abbreviations: A_H, Hamaker constant; BT, Bartsch test; CMC, critical micellar concentration; C_nEO_m, alkyl polyoxyethylene; C_S, surfactant concentration; d_h, hydrodynamic diameter; e, elementary charge; E_A, activation energy; EO, ethylene oxide; FRM, foam rise method; GC, gas chromatography; h, film thickness; H-bond, hydrogen bond; HPLC, high performance liquid chromatography; I, light intensity; IS, ionic strength; k_B, Boltzmann constant; L, wavelength; MBPM, maximum bubble pressure method; n, refractive index; n_0, electrolyte number concentration; N_A, Avogadro number; P_C, capillary pressure; Π_{MAX}, maximal disjoining pressure; R, universal gas constant; SDS, sodium dodecyl sulfate; T, temperature; t, time; t_u, universal surface age; V_A, volume of air; X_{CMC}, surfactant molar fraction at CMC; α, excluded area per molecule; ΔG_m^0, standard free energy of micellization; η, viscosity; θ_{CMC}, surface coverage; κ^{-1}, Debye length; λ, conductivity; π_S, surface pressure; σ, surface tension; σ_0, surface tension of pure solvent; Ψ_S, electrical surface potential; Γ, surface concentration.

* Correspondence to: Department of Chemical and Pharmaceutical Engineering, Faculty of Chemistry and Pharmacy, Sofia University, 1 James Bourchier Ave, Sofia 1164, Bulgaria.

E-mail address: SC@LCPE.UNI-SOFIA.BG (S. Tcholakova).

https://doi.org/10.1016/j.colsurfa.2024.133844
Received 22 January 2024; Received in revised form 10 March 2024; Accepted 29 March 2024
Available online 30 March 2024

concentrations for foams with bigger bubbles. The addition of 6 M urea, resulted in increased adsorption without any effect on foam stability for L1695, whereas it decreased the adsorption and foam stability for Brij L23. The comparison of relative foamability *vs.* dynamic surface coverage revealed that a lower threshold surface coverage is required to increase the foamability of L1695 (≈ 80%) compared to Brij L23 (≈ 95%). This difference is explained by the action of weak electrostatic repulsion and the adsorption of sucrose diesters on the bubble surfaces when L1695 surfactant is used. The higher stability of L1695 foams under all studied conditions is attributed to the formation of a denser adsorption layer due to the adsorption of sucrose diesters. The diesters prevent the formation of weak spots within the foam films, even at high temperatures. This work contributes to the advancement of the foam field by demonstrating that a mixture of sucrose mono and diester surfactants can be highly effective in forming stable foams at higher temperatures and in the presence of urea. Both factors (higher temperature and 6 M urea) have negative effect on Brij L23 foams, while they have no significant effect on L1695 foams with smaller bubbles.

1. Introduction

Nonionic surfactants find applications in various industries such as food and beverages, home and personal care products, and pharmacy [1–5]. The nonionic polyoxyethylene alkyl ether surfactants, denoted as C_nEO_m, where n is a number of C-atom in hydrophobic tail and m is the number of EO groups in hydrophilic head group, have been extensively studied in the literature for their surface, aggregation, film, and foam properties [6–12]. It was shown that the critical micellar concentration (CMC) for $C_{12}EO_m$ surfactants remains relatively constant for values of m ranging from 4 to 25 [12]. The CMC exhibits a minimum at temperature ≈ 50°C for homologues with m between 4 and 8 [9]. The surface pressure at CMC decreases as the number of EO groups or the temperature increases [9].

The foamability increases, while the foam stability decreases with the number of EO groups for foams formed from 1 mM $C_{12}EO_m$ solutions in the Ross Miles test [6]. The improved stability of foams formed by mechanical stirrer at high surfactant concentrations from $C_{12}EO_m$ homologues with a smaller number of EO groups (m = 3 or 5) was attributed to the adsorption of lamellar liquid crystalline phases on the bubble surface and their presence in the continuous phase [10]. Further enhancement of foam stability is reported in [11] for surfactants with a small number of EO groups and a longer chain length, such as $C_{16}EO_2$ or $C_{18}EO_2$ [11].

Sucrose alkyl esters, considered as biodegradable and biocompatible surfactants, are widely used in the food industry [1,11,13–15]. These surfactants contain a mixture of sucrose mono-, di-, and triesters, whose ratio affects the foam properties [16]. A commercial sucrose dodecyl ester mixture of monoesters and diesters, L1695, exhibited enhanced foamability and stability compared to its individual components (monoesters and diesters) [16]. A 4:1 molar ratio mixture of monoester and diester showed similar foam performance to L1695 [16]. However, the authors noted no significant effect of the added diesters on the surface and foam film properties of monoesters, attributing the enhanced foaming of the mixture to interactions between monoesters and diesters within the bulk [16]. Van Kempen et al. [17] showed that oligofructose mono-esters (containing 2–8 fructose units) with intermediate fatty acid chain lengths (C_{10}-C_{16}) led to the highest foam stability in a bubbling method compared to diesters or monoesters with different chains (C_4-C_8 and C_{18}). In the same study [18] it was shown that C_{12} sucrose ester produces foams with smaller in size bubbles compared to C_{16} and C_8 sucrose esters.

The temperature significantly impacts the properties of nonionic surfactants by decreasing the degree of micelle hydration [18–20]. The decrease of hydration numbers from 4.2 at 20 °C to 2.9 at 60 °C is determined experimentally for 0.01 M $C_{12}EO_6$ solution [20]. Molecular dynamic simulations suggest that this dehydration involves a collective reorganization of the water-water hydrogen-bond network in the palisade layer and on the oil core surface of the micelle, but the latter effect being more important [18].

The increase in temperature also has a significant effect on the foam properties [21–23]. Wang et al. [21] demonstrated that the stability of foams formed by the bubbling method decreases with increasing temperature for all studied surfactants (anionic, cationic, nonionic, and amphoteric). Rezaei et al. [22] showed that the stability of foams formed from surfactant-silica suspension also decreases with temperature increase. Oetjen et al. [23] demonstrated that stability decreases with temperature for fresh and UHT treated milk foams.

The role of hydrogen bonds (H-bonds) for foam stability has been extensively studied [24–35]. H-bond formation within the adsorption layer has been proposed to explain the improved stability of foams formed from dodecanoyl glycinate, as compared to dodecanoyl sarcosinate [29], the maximal stability around pKa for a series of fatty acids [30] and for dodecyldimethylamine oxide [26], for the improved stability of n-dodecyl-β-D-maltoside foams as compared to $C_{12}E_6$ foams [31] and of 1-*O*-dodecyl diglyceryl ether compared to $C_{12}E_5$ [36]. The formation of H-bonds was also shown to be responsible [32,33] for the very high surface elasticity and viscosities of escin adsorption layers [34,35], and for the formation of very stable saponin-stabilized foams with respect to Ostwald ripening [37]. Sugar-sugar H-bond formation is considered to be enthalpy-driven [27].

Urea, known as a denaturant for proteins, has been shown to impact the critical micellar concentration for both ionic and nonionic surfactants [38–42]. The mechanisms behind this effect are not fully understood, but there are two distinctive explanations have been proposed in the literature: (1) weakened hydrophobic effect due to lower interfacial tension between surfactant tail and water molecules in presence of urea and (2) reducing the degree of water-water hydrogen bonding without replacing these interactions by strong urea-water hydrogen bonds [38–43]. Studies indicate that urea replaces water molecules in the hydration shell, leading to an increase in CMC for various nonionic surfactants [40–42]. It is well established in the literature, that the increase of urea concentration is analogous to the reduced temperature for the micellar properties of nonionic surfactants [42]. However, with respect to the foaming properties of nonionic surfactant Triton X-100, it was shown that the addition of urea was analogous to increasing the temperature – the foam stability decreased by adding urea and by increasing the temperature [44]. Therefore, it is valuable to compare the effect of temperature and urea on the surface, film and foam properties of nonionic surfactants and to clarify what is the reason for their different effects on micellar and foam properties.

In our previous studies [45,46], a detailed theoretical approach was developed to analyze the foamability of surfactant solutions in different foaming methods. For each foaming method, the time scale for bubble generation was determined. The dynamic surface tension at this time scale was measured and was used to calculate the surfactant adsorption on the bubble surface at the moment of bubble formation. The maximal adsorption was determined from the measured surface tension isotherms. The dynamic surface coverage defined as the ratio between the surfactant adsorption at moment of bubble formation and maximal possible adsorption was calculated. The universal master curves between foamability and dynamic surface coverage were established [45,46]. The foamability begins to increase at a dynamic surface coverage of ≈ 30% for ionic surfactants and 95% for nonionic surfactants with

ethoxylated head groups [45]. A recent extension of this approach demonstrated its applicability to predict the foamability of polymeric solutions, considering also the respective long-range steric repulsion which decreases the required dynamic surface coverage for starting the foamability to 80% [47].

To the best of our knowledge, there is no information about the impact of temperature or hydrogen bonds on the surface, film, and foam properties of alkyl sucrose esters. Therefore, the current study aims to: (1) Assess the applicability of the previously developed approach in [45, 46] for describing the foamability as a function of dynamic surface coverage for foams formed at different temperatures and in the presence of 6 M urea; (2) Determine the foam stability at different temperatures and in the presence of 6 M urea for nonionic surfactants capable of forming intersurfactant hydrogen bonds, such as L1695; (3) Clarify the impact of temperature and 6 M urea addition on the surface and film properties of L1695 and Brij L23.

To achieve those aims, experiments were conducted with two C_{12} surfactants – dodecyl sucrose ester (L1695) and dodecyl polyoxyethylene alkyl ether (Brij L23). We chose these surfactants as they have significantly different head groups and ability to form intermolecular hydrogen bonds. The experiments were carried out at temperatures ranging from 25°C to 60 °C, and at 25 °C in a highly concentrated urea solution (6 M). Adsorption and foam film properties were characterized, and the respective results were used to explain the foamability and foam stability of these solutions in two foaming methods: the Bartsch test (denoted hereafter as BT for shortness) and the foam rise method (denoted hereafter as FRM), also known as the bubbling method.

2. Materials and methods

2.1. Materials and procedure for solution preparation

Dodecyl sucrose ester L1695 was obtained from Ryoto. According to the producer, it contains 95% lauryl alkyl chains, 80% monoesters and 20% di-, tri- and polyesters [48]. Brij L23 was obtained from Sigma-Aldrich and according to its producer it contains mono dodecyl ethers with mean number of EO groups in the head group of 23. Molecular weights of 565 g/mol and 1198 g/mol were used for L1695 and Brij L23, respectively.

Urea (> 99.5%) was obtained from Riedel de Haen (Honeywell International Inc., USA). All chemicals were used as received without any further purification. All solutions were prepared using deionized water obtained by Elix 3 system (Merck-Millipore Inc., USA).

L1695 and Brij L23 surfactant solutions were prepared by stirring the surfactant/water mixture at 60°C for 30 min using a magnetic stirrer. For high-urea content experiments, 6 M urea solution was first prepared by adding urea to water to yield 33 wt% concentration. This mixture was stirred overnight at room temperature using a magnetic stirrer. The desired amount of surfactant was then weighed and added to the 6 M urea solution, and prepared as described above. All concentrations are given as weight percentages relative to the solution weight. All L1695 solutions and Brij L23 solutions were clear in the investigated conditions and were used within 48 hours after their preparation. All chemicals used in the chemical analyses were of analytical grade.

2.2. HPLC and GC procedures for analysis of L1695 chemical composition

2.2.1. Gas chromatography (GC)

L1695 was weighed on an analytical scale and transferred into a glass vial. After that a 3 mL of 3.33 M alcoholic potassium hydroxide (prepared with 8:2 ethanol/water) was added. The sample was stirred at 60°C for 4 hours, and the ethanol-water mixture was then removed by evaporation using compressed air. The resulting saponified fatty acids, in a dry state, were reconstituted in water and the pH of the solution was adjusted to a value of 2 by addition of 2 M HCl. The fatty acids were then extracted with 10 mL chloroform with pre-dissolved pentadecanoic acid as internal standard. For the derivatization, prior to injection into the GC column, 400 µL of the sample was combined with 200 µL of pyridine and 200 µL of N,O-bis(trimethylsilyl)trifluoroacetamide. This mixture was then heated to 60 °C for 1 hour, and then diluted 19x times with *iso*-octane.

The GC analysis was performed on Agilent 8890 apparatus (Agilent technologies, Santa Clara, CA, USA), connected to an autosampler 7693 A. An Agilent DB-5HT capillary column was used, having the following specifications: (5%-Phenyl)-methylpolysiloxane, 30 m length, I.D. 0.32 mm, 0.1 µm film thickness. An injection volume of 1 µL and cold on-column injection was used. The oven was programmed in the following way: start at 60 °C, hold 1 min, the ramp to 180°C at 10 °C/min, hold 0 min, ramp to 350°C at 30 °C/min, hold 10 min. The sample analysis time was 29.5 min. The flame ionization detector was operated at T = 380 °C. Helium at a constant flow of 2 mL/min was used as a carrier gas. Hydrogen, air and nitrogen (make-up gas) were used as detector gases. The concentrations of the fatty acids were calculated using pentadecanoic acid as an internal standard.

2.2.2. High performance thin liquid chromatography (HPLC)

The HPLC analysis was carried out on a Shimadzu apparatus, equipped with LC-40DX3 delivery module and evaporative light scattering detector, operating at 40°C, 350 kPa, Gain 8. The analytical column was Waters X-Bridge, 150 ×4.6 mm, 5 µm, 130 Å, operating at 45 °C. Gradient elution was used with flow rate of 1 mL/min. (A) Water (B) Methanol were used in the following sequence: 0 min - 40% B, 20 min - 70% B, 30 min - 75% B, 45 min - 100% B, 60 min - 100% B, 60.1 min - 40% B, 65.0 min - 40% B.

2.3. Determination of micelle size

The size of the micelles, formed in 1 wt% of L1695 and Brij L23 solutions, was measured at different temperatures using dynamic light scattering on Zetasizer Nano® ZS, Malvern Panalytical. The required temperature was controlled by apparatus internal chamber. The temperature was adjusted with accuracy of ± 0.1°C. The mean volume diameter of the micelles, d_h, is given in the text below. The reported results at a given temperature are averaged from 6 measurements of two independently prepared solutions.

2.4. Surface tension measurements

The surface tensions were measured by using Krüss K100 tensiometer equipped with DS110 micro-dispenser (Krüss GmbH, Hamburg, Germany).

For construction of surface tension isotherms, a Du Nouy ring was used for the measurements. For calculation the dynamic surface coverage on the bubble surface in foam rise test, the surface tension was measured by using Wilhelmy plate. In both experiments, the temperature was kept within 0.2 °C during the experiment by thermostat (Julabo GmbH, Germany) and thermostatic pump CORIO CD-200 F to circulate the thermostated water.

For several selected concentrations of L1695, the surface tension was measured using the pendant drop method on DSA30 (Krüss GmbH, Germany), equipped with thermostatic cell TC40. Experiments were conducted at 25 °C and 50 °C ± 1 °C and repeated twice.

Dynamic surface tension was measured by the maximum bubble pressure method (MBPM) with a processor-controlled bubble pressure tensiometer Krüss BP2 (Krüss GmbH, Hamburg, Germany) at fixed temperatures of 25.0 °C, 40.0 °C, 50.0 °C and 60.0 °C, kept by circulating water using a CORIO CD-200 F thermostatic pump (Julabo GmbH, Germany) with accuracy of 0.2 °C. Hydrophobized glass capillaries with a hydrophilic tip were used for all measurements and their diameter was measured before each set of experiments. The reported results are from single measurement for each concentration.

2.5. Foam film properties

A capillary cell was used to observe the behavior of thin foam films [49]. The films were formed in a capillary with radius of 1.25 mm by sucking out the solution through a side orifice. The films were observed in reflected light with optical microscope Leica DM RXE (Leica Microsystems, GmbH; Wetzlar, Germany) equipped with long-distance objective Nplan 20x/0.4, CCD camera (Sony SSC-C370P) and 5.1 M Video Biological Microscope Digital Camera 55FPS LCMOS. The typical radius of the foam films formed in this capillary cell was ≈ 0.125 mm. The temperature was controlled using a steel cell-holder with inner water circulation using a CORIO CD-200 F thermostatic pump (Julabo GmbH, Germany). The top glass cover was heated to avoid the formation of condensation droplets. The solution temperature was monitored using a type K thermocouple probe and a UT325 thermometer (Uni-Trend Technology co. Ltd., China). From the intensity of the reflected light, the foam film thickness was determined [49]. The film thinning pattern and the stability of the foam films were studied in a closed cell to suppress the water evaporation from the films. Each film was observed for 10 min after its formation. At least three independent films were observed for a given concentration at a given temperature. The temperature was controlled with accuracy of 1 °C.

The film thickness, h, was determined based on the obtained images, after converting them to gray scale, and using the following expression [49]:

$$h = \frac{L}{2\pi n} \times \arcsin\left(k\pi + \sqrt{\frac{I - I_{\min}}{I_{\max} - I_{\min}}}\right)$$

Where L is the wavelength of the incident light (for white light, the peak is around 565–580 nm), n is the film refractive index, I is the intensity of the reflected light from the film, I_{max} is the maximal intensity of the reflected light of white film, I_{min} is the minimal intensity of the reflected light after film breakage, k is the order of interference maximum (0,1,2, etc). Intensities are determined using the Corel Photo Paint software.

2.6. Foamability and foam stability

The foamability of the studied solutions was determined in Bartsch test (BT, fast-foaming method) and in foam rise method (FRM, slow-foaming method). In Bartsch test there is a rapid expansion of the solution surface during the air entrapment, whereas the bubbles in foam rise method are formed more slowly and they travel through the solution where additional adsorption of surfactant can occur before reaching the other bubbles in the top of the foam column.

2.6.1. Bartsch test

A glass cylinder of 120 mL, filled with 10 mL surfactant solution, was shaken using automated Bartsch test for 100 cycles, at shaking period of 1.23 s (frequency = 0.813 s^{-1}). The method is described in details in Ref. [45]. To control the temperature, we used a 3000 W blow heater, regulated by PID thermocontroller and AC phase regulator, connected to an in-chamber type K thermocouple probe. Experiments were conducted at T = 25, 40, 50 and 60 ± 1 °C. At least three different cylinders were used to determine the foamability under given conditions.

2.6.2. Foam rise method

Foam was generated by blowing the air through a 1.5 cm diameter filter paper with pores of 8–12 μm size into 20 mL of the surfactant solution, contained in a glass column. The column dimensions are: 2.8 cm internal diameter and 20 cm total height. An air flow rate of 0.38 ± 0.02 L/min was maintained for 15 s. Experiments were conducted at T = 25, 40, 50 and 60 ± 1 °C and temperature was controlled by immerging the glass column inside a thermoregulated water bath. Foam height was monitored by visual observation every minute for 10 min after air sparging was stopped. Each experiment was repeated three times.

2.6.3. Characteristics of foamability and foam stability

To characterize the foamability of the studied solutions, the volume of entrapped air, V_A, was determined by subtracting the solution volume from the total volume (solution + foam).

The foam stability was evaluated after stopping the agitation in BT or after stopping the air supply in FRM. The remaining volume of entrapped air was monitored by visual observation every 2 min for 10 min. The ratio between the air, remaining in the foam 10 min after stopping the agitation, and the initial amount of air entrapped during the shaking period is used to characterize foam stability.

2.7. Viscosity measurements

The viscosity of the solutions was measured with a modular compact rheometer MCR-302e (Anton Paar, Austria), using cone and plate geometry with a diameter of 40 mm (cone angle 1°, truncation gap 78 μm). Measurements were conducted at 25.0, 40.0, 50.0, and 60.0 °C, and samples were equilibrated for 3 min before each measurement. The rheological test in a steady shear regime was performed by varying the shear rate logarithmically and stepwise from 0.01 s^{-1} to 500 s^{-1}. The viscosity was monitored as a function of shear rate. For reproducibility, each measurement was repeated twice, and the average results are presented.

3. Experimental results and discussions

In Section 3.1, the chemical composition of used L1695, determined by GC and HPLC analysis, and the bulk properties (viscosity and micelle size) of 1 wt% aqueous solutions, are described. Section 3.2 presents the measured surface tension isotherms and the determined characteristics of the adsorption layers, which are used in Section 3.3 to calculate the dynamic surfactant adsorption from the measured dynamic surface tensions. The behavior of foam films is described in Section 3.4. Finally, Section 3.5 summarizes the results from the foaming experiments and their interpretation.

3.1. Surfactants' composition and bulk properties of 1 wt% solutions

The chemical composition of sucrose ester L1695 was analyzed by HPLC to determine the monoester-to-diester ratio, and through GC after hydrolysis to establish the fatty acid-chain length ratio. L1695 comprises 87% monoesters and 13% diesters with chain-length composition of > 99% C12, in good agreement with the information provided by the manufacturer [48].

The measured shear stress *vs.* shear rate dependencies for solutions with surfactant concentration, C_S, of 1 wt% exhibit Newtonian behavior under all conditions studied. The measured viscosities are shown in Fig. 1 A and it is seen that the viscosity decreases with the increase of temperature and increases upon addition of 6 M urea. The latter effect can be attributed to the higher viscosity of the urea-water mixture compared to water alone (1.403 mPa.s *vs.* 0.89 mPa.s at 25°C) [50].

The relative viscosity is defined as the ratio between the viscosity of the surfactant solution and the viscosity of the continuous phase in which surfactant molecules are dissolved (water for aqueous solutions without urea and 6 M urea solution for urea-containing solutions). The relative viscosity increases from 1.4 to 1.5 with the rise in T from 25 to 40 °C and remains constant thereafter. This suggests that the presence of micelles has the least impact on viscosity at T = 25 °C. However, the relative viscosity of the solutions, containing 6 M urea, is very similar to that, determined for water solutions without urea, suggesting that the micelles have a comparable effect in both water and water-urea solutions.

Following the approach developed in [51,52], the dependences of ln (η) *vs.* 1/T were plotted for two studied solutions, see Figure S1 in SI.

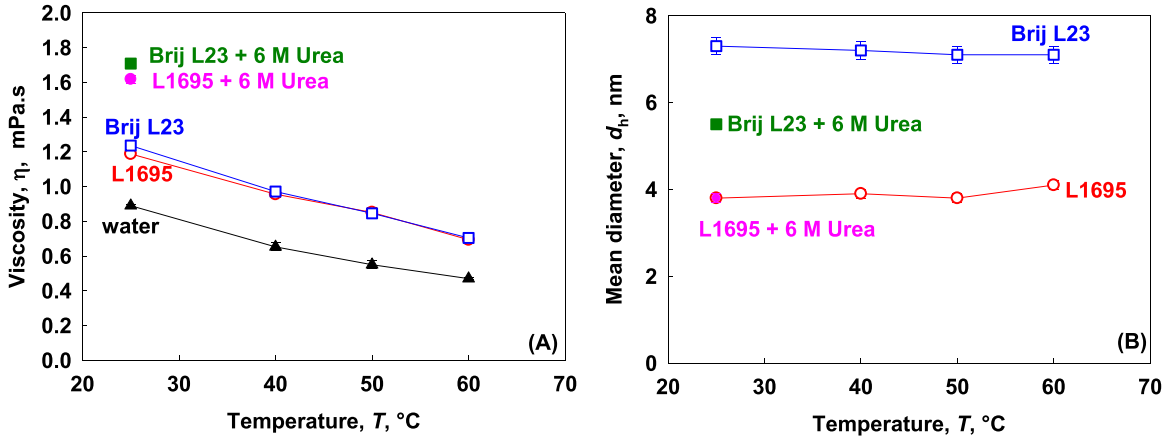

Fig. 1. (A) Solution viscosity, η and (B) Mean hydrodynamic diameter of the micelles, d_h, measured by dynamic light scattering as a function of temperature, T, for 1 wt% solutions of Brij L23 (squares) and L1695 (circles) in water (empty symbols) and in 6 M urea solution (full symbols).

From the slope of the curve, the activation energy (E_A), required to overcome the attractive forces, binding the molecules to their neighbors, was determined and compared to the activation energy, known for water molecules in the absence of added surfactants. The presence of Brij L23 molecules in the solution results in a reduction of E_A for water molecules from 15.5 kJ/mol [52] to 13.2 kJ/mol. On the other hand, the presence of L1695 micelles leads to a further decrease down to 12.4 kJ/mol. This comparison indicates that the presence of micelles diminishes the attractive forces between water molecules in the bulk.

The hydrodynamic diameters, d_h, of the micelles in 1 wt% solutions remain relatively constant with T for both studied surfactants, see Fig. 1B. However, the average size of L1695 micelles is twice smaller compared to Brij L23 micelles (7.3 nm vs 3.8 nm) at $T = 25$ °C. The presence of 6 M urea significantly decreases d_h for Brij L23 micelles from 7.3 nm to 5.5 nm, whereas it has no effect on L1695 micelles.

The measured sizes for Brij L23 are in good agreement with previously reported results for Brij 35 [53]. Note that Brij 35 and Brij L23 are different names for surfactants of similar structures of $C_{12}EO_{23}$. The mean micelle size increases with T for nonionic surfactants close to the cloud point [41], however, the studied temperature range is well below the cloud point of Brij L23, which is $\geq$ 100 °C. As a consequence, the increase of temperature has almost no effect on the micelle size for Brij L23. The microviscosity in the palisade layer of Brij 35 micelles was found to decrease from 17.1 mPa.s to 9.4 mPa.s when increasing T from 25 to 50 °C [54], suggesting weaker binding of water molecules to the EO groups at higher temperature.

The presence of 6 M urea leads to a decrease of d_h from 7.3 to 5.5 nm for Brij L23, in accordance with results for $C_{12}EO_6$ [41]. This effect is explained with a altered interactions between the EO groups in hydrophilic head and water in the presence of urea [41]. Indeed, the hydration shell decreases in the presence of urea [40,41]. No significant impact of urea was observed for L1695 micelles, suggesting that the water-sugar group interactions are less affected in that case.

Literature data indicate that the radius of the hydrophobic core of Brij 35 micelles is $\approx$ 1.64 nm [55,56]. Nearly spherical micelles are formed in Brij 35 solutions at studied concentrations [55,56]. Assuming spherical micelles for both surfactants and a similar hydrophobic core radius to that of Brij 35, the palisade layer thickness can be calculated by subtracting from d_h the core diameter ($\approx$ 3.28 nm) and divided by two. The estimated palisade layer thicknesses are $\approx$ 2 nm for Brij L23, which agrees well with data reported in Ref. [56] and $\approx$ 0.26 nm for L1695 micelles. Therefore, the substantial difference in d_h for Brij L23 and L1695 micelles is attributed to the formation of thicker palisade layer of EO groups for Brij L23 micelles compared to palisade layer of L1695 micelles.

Interestingly, the presence of urea molecules in the solution decreases the thickness of palisade layer for Brij L23 micelles from 2 nm down to 1.11 nm. This effect can be explained by incorporation of urea molecules in the palisade layer in accordance with data reported in Ref. [42], which changes the conformation of EO groups chain and decreases the palisade layer thickness. No such effect is observed for L1695, because the palisade layer is very thin and the urea molecules are not incorporated therein.

In summary, these experiments reveal no significant difference in the viscosity of Brij L23 and L1695 solutions, but a significant difference in the micelle size. The micelles in Brij L23 are about twice larger than those in L1695 due to the strong hydration of the EO groups. The addition of urea does not affect significantly the properties of L1695 micelles, while it has a significant impact on the size of Brij L23 micelles, possibly by replacing water molecules in the palisade layer and decreasing the palisade layer thickness of hydrated head groups due to possible change in the conformation of EO groups chain.

3.2. *Properties of equilibrium adsorption layers*

The properties of the adsorption layers, within the temperature range of 25°C to 60°C, were characterized by measuring the surface tension, σ, of the surfactant solutions using the du Nouy ring method. In our previous studies [45,46], the equilibrium surface tension was determined from the intercept of σ *vs.* $1/t^{1/2}$, where t is the time, assuming diffusion-limited adsorption [57]. In the current study, L1695 is a mixture of mono and di-esters, each with significantly different diffusion coefficients. At shorter times, monoesters adsorb on the interface due to their higher concentration and higher diffusion coefficient, but over an extended period, the diesters gradually replace the monoesters at the interface due to their higher energy for adsorption and slower rate of desorption. Consequently, the surface tension does not reach a plateau value even after 1 hour of measurement, particularly at elevated temperatures where the adsorption of diesters is easier, see Figure S2 in SI.

The replacement of monoesters with diesters is crucial for the prolonged foam stabilization. However, for foamability, the role of diesters is limited as they cannot adsorb on the bubble surface at short times due to their slow diffusion toward the interface. Therefore, it is reasonable to assume that during the foaming process, the prevailing species in the adsorption layers formed on the bubble surfaces, are molecules that can be adsorbed within the time scale of foam generation. Our previous studies show that for the FRM, the characteristic time scale is $\approx$ 50 s [46], whereas for the Bartsch test, it is $\approx$ 10 ms [45]. Hence, for calculating the properties of the quasi-equilibrium adsorption layers in the current study, we use the surface tensions measured after 100 s, which is twice longer than the characteristic time for foam generation in the FRM and 10^4 times longer than the characteristic time for foam

generation in the BT.

The determined isotherms are analyzed to extract the key characteristics of the studied surfactants: (1) critical micellar concentration, CMC; (2) surface tension at CMC, σ_{CMC}; (3) surfactant adsorption at CMC, Γ_{CMC}; (4) excluded area per molecule, α, and (5) surface pressure at CMC, π_{CMC}. Surface tension data below CMC were used to calculate the surfactant adsorption at CMC, Γ_{CMC} (μmol/m^2), by using Gibbs' equation [57]:

$$\frac{d\sigma}{d\ln C_S} = -RT\Gamma_{CMC} \quad (1)$$

In this equation Γ_{CMC} is the surfactant adsorption at CMC, σ is the measured surface tension after 100 s, R is the universal gas constant, T is the temperature, and C_S is the bulk surfactant concentration. The excluded area per molecule, α, was calculated from the measured values of σ_{CMC} and Γ_{CMC}, assuming that adsorption can be described by Volmer equation [11]:

$$\alpha = \frac{1}{N_A\Gamma_{CMC}}\left(1 - \frac{RT\Gamma_{CMC}}{\sigma_0 - \sigma_{CMC}}\right) \quad (2)$$

where N_A is Avogadro number and σ_0 is surface tension of the pure solvent, which is 72.0; 69.6; 67.9; or 66.2 mN/m at 25 °C, 40 °C, 50 °C or 60 °C, respectively, for water, and 74.8 mN/m for 6 M urea solution at 25°C.

The characteristics for Brij L23, utilizing the equilibrium surface tension, σ_{EQ}, determined from the intercept of σ *vs.* $t^{-1/2}$ and σ measured after 100 s, are compared in Figure S3 in SI. The analysis reveals that there is no significant difference between the extracted parameters from different adsorption isotherms for this surfactant. This suggests that the composition of the adsorption layer does not change significantly over time. However, this is not the case for L1695, where notable differences are observed not only in the values of CMC, but also in all other characteristics. In that case, the composition of the adsorption layer undergoes significant changes over time.

The surface tension isotherms, based on σ measured after 100 s, are presented in Fig. 2. A shallow minimum is observed under all studied conditions (different T and ± 6 M urea) for both surfactants, indicating that some of the most surface-active substances are solubilized in the micelles after their formation. There is a well-defined region, in which the surface tension decreases linearly with $\ln C_S$, from which Γ_{CMC} was determined, using Eq. (1). The cross point between the linear dependence of σ *vs.* $\ln C_S$ with the minimal surface tension measured, under given conditions, is used to calculate CMC. The extracted characteristics are shown in Fig. 3.

The CMC is significantly higher for L1695 compared to Brij L23 in the entire temperature range, and decreases with the increase of temperature for both surfactants, see Fig. 3B. The observed CMC decrease for Brij L23 with temperature aligns well with literature data for Brij 35, where it was demonstrated that CMC decreases from 43 μmol/L down to 34 μmol/L upon increase of temperature from 35 °C to 50 °C [58]. However, the presence of 6 M urea in the aqueous solution has opposite effect on CMC for L1695 and Brij L23: CMC decreases more than 10 times for L1695, from 345 μmol/L down to 32 μmol/L, whereas it increases more than 4 times for Brij L23, from 48 μmol/L up to 210 μmol/L, see Fig. 3B. The CMC increase upon addition of 6 M urea for Brij L23 agrees well with the results reported for $C_{12}EO_8$ [41], showing that the molecules rather stay in contact with the water-urea mixture instead of forming micelles. The observed effect of urea on L1695 CMC is opposite to the well-established effect on other ionic and non-ionic surfactants [38–44]. This is probably due to the fact that urea is

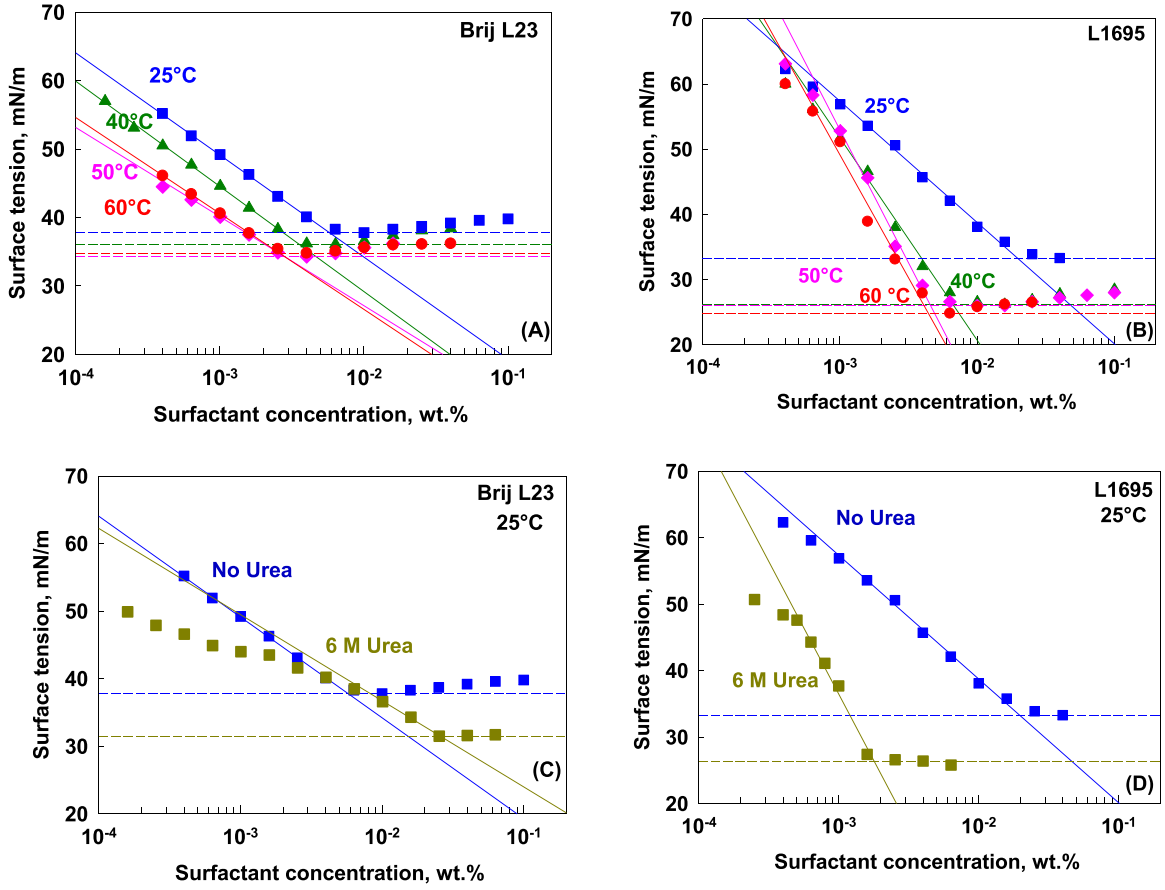

Fig. 2. Surface tension isotherms for (A,C) Brij L23 and (B,D) L1695 measured at (A,B) different temperatures and (C,D) in presence and in absence of 6 M Urea at T = 25 °C. Surface tension values, σ, are taken after 100 s using a du Nouy ring method.

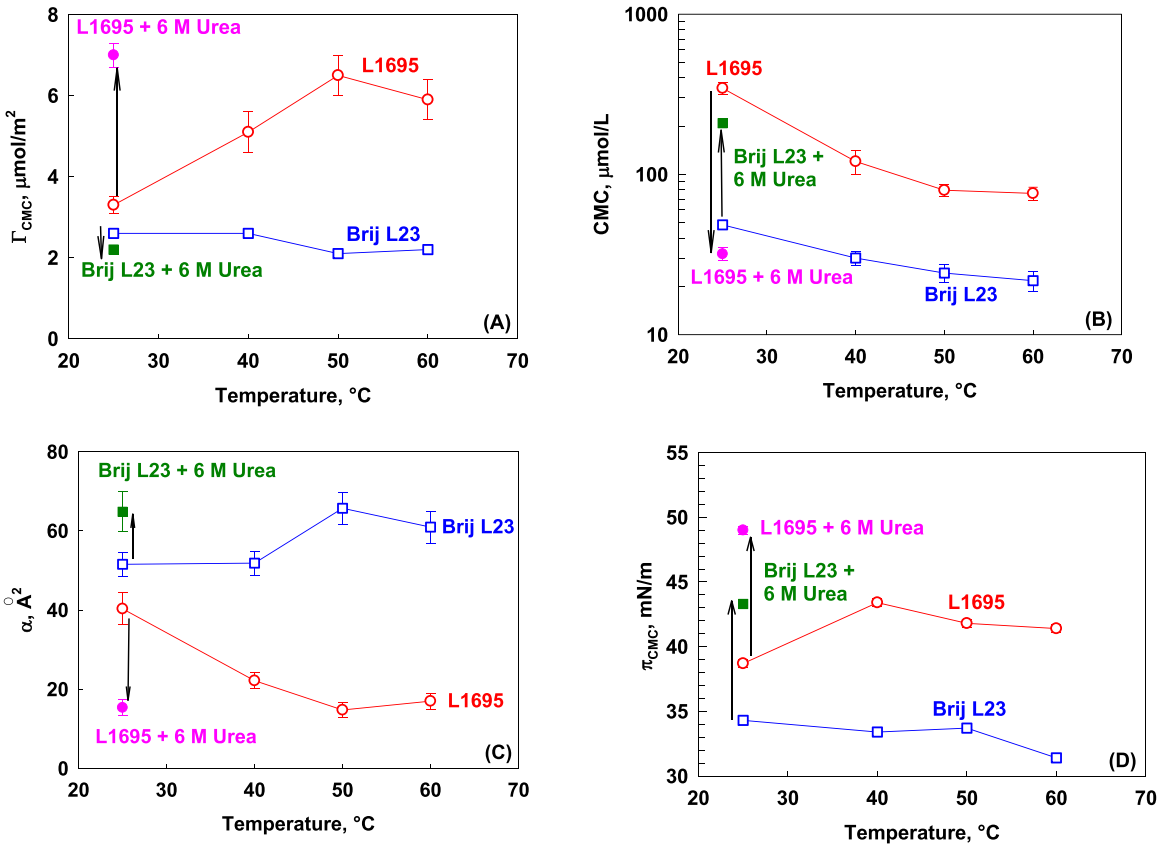

Fig. 3. (A) Surfactant adsorption at CMC, Γ_{CMC}; (B) Critical micellar concentration, CMC; (C) Excluded area per molecule, α; (D) Surface pressure at CMC, π_{CMC}, as a function of temperature for Brij L23 (squares) and L1695 (circles) without (empty symbols) and with 6 M urea (full symbols).

unable to replace the water molecules in the hydration shell of L1695 micelles, as it does in Brij L23 micelles. The presence of urea in the solution is shown to strengthen the water structure, resulting in stronger water-water hydrogen bonds and a more rigid occupation of tetrahedral coordination positions, as demonstrated by molecular dynamic simulations in Ref. [59]. Therefore, the CMC decreases with the presence of urea when it does not incorporate in the hydration shell (*e.g.*, L1695), and increases when it does (*e.g.*, Brij L23).

The determined CMC values were used to calculate the micellar characteristics, following the approach developed in Ref. [60] for the standard free energy of micellization, ΔG_m^0:

$$\Delta G_m^0 = RT \ln X_{CMC} \tag{3}$$

Here, X_{CMC} is the surfactant molar fraction at CMC, calculated as $X_{CMC} = CMC/55.5$. The resulting values of $-\Delta G_m^0$ for Brij L23 increased from 35 kJ/mol to 41 kJ/mol with an increase in T from 25 °C to 60°C, which is in good agreement with literature data, where an increase from 35 kJ/mol to 38 kJ/mol was reported upon increase of T from 35 °C to 50 °C [58]. The latter effect is explained in Ref. [58] by easier approaching of the molecules in the micelles at higher temperature as EO groups get dehydrated. For L1695, the $-\Delta G_m^0$ value increased from 30 kJ/mol to 37 kJ/mol for $T = 25$ °C to 60 °C, highlighting the role of the sugar moiety hydration for this rise of standard free energy of micellization at higher temperature.

Temperature rise from 25 °C to 60 °C has adverse effect on surfactant adsorption at CMC, Γ_{CMC}: it decreases from 2.6 μmol/m^2 to 2.2 μmol/m^2 for Brij L23, and increases from 3.3 μmol/m^2 up to 6.0 μmol/m^2 for L1695, see Fig. 3 A. In the case of Brij L23, this is in good agreement with results obtained for the air-water interface using Brij 35 [61], whereas the opposite trend is usually reported for the solid-water interface [62, 63]. The decreased adsorption with T on the air-water interface is somewhat surprising because, according to the conventional view, higher temperature should result in a decrease in the hydration shell and in the respective steric repulsion between the head groups, leading to higher adsorption with T, as observed for the solid-water interface. In the case of L1695, the significant increase in Γ_{CMC} with T agrees more with the conventional expectation, and is additionally related to the faster adsorption of diesters at higher temperatures, forming a denser adsorption layer with a smaller hydration shell of sucrose head groups.

In the presence of urea, Γ_{CMC} increases for L1695 up to its maximal value of 7 μmol/m^2, indicating that L1695 molecules prefer to form micelles or adsorb on the air-water interface, instead of staying as monomers in the solution. This behavior is opposite compared to the one observed for Brij L23 molecules which prefer to stay dissolved in the urea-water mixture instead of forming micelles or adsorbing on the air-water interface. As a consequence, CMC increases and Γ_{CMC} decreases for Brij L23 in 6 M urea solution.

The calculated excluded area per molecules, α, is larger for Brij L23 compared to L1695 under all conditions studied, see Fig. 3 C, indicating looser adsorption layers with Brij L23. This significant difference in α denotes higher repulsion between Brij L23 molecules than between L1695 molecules within the adsorption layer. Diesters in L1695 most likely facilitate the formation of a denser layer for this surfactant. Moreover, the higher adsorption could also be related to the formation of intersurfactant H-bonds in L1695 adsorption layer which could not be realized in Brij L23 layers.

Again, opposite effects are observed on α for both surfactants upon addition urea or upon increasing T. The excluded area per molecules increases from 0.52 to 0.61 nm^2 with T for Brij L23, which is similar to the effect of urea incorporation within the adsorption layer. In the case of L1695, however, it decreases from 0.40 to 0.17 nm^2 upon increasing T from 25 to 60 °C. The latter value is very close to the cross section of frozen surfactant tails [64], indicating the formation of condensed layers

on the air-water interface at 50 and 60°C.

The calculated surface pressures at CMC, π_{CMC}, shown in Fig. 3D, reveal significantly higher values for L1695 compared to Brij L23, in agreement with the higher adsorption of L1695. Similar trend is observed in presence of urea for this surfactant. The increase in π_{CMC} value for Brij L23 upon urea addition is probably related to urea incorporation close to the interface. This could explain the distinct shape of the surface tension isotherm curve for this system, as shown in Fig. 2C.

From these series of experiments, it can be concluded that both an increase in T and the presence of 6 M urea result in the formation of looser adsorption layers for Brij L23, and denser adsorption layers for L1695. Regarding the evolution of CMC, it decreases for both surfactants with the increase in temperature, while urea has adverse effects: it increases the CMC for Brij L23 and decreases it for L1695. Those results can be explained as follows: (1) the decrease in CMC with T is related to the weakening of steric repulsion between the hydrated head groups; (2) the increase in CMC for Brij L23 upon addition of urea is related to the substitution of water molecules with urea molecules, weakening the hydrophobic attraction between the surfactant tails. In L1695, stronger H-bonds between the sugar head group and water molecules prevent water from being substituted with urea. As a consequence, urea remains in the bulk water, facilitating its structuring, and strengthening the hydrophobic interactions between L1695 molecules. (3) The higher adsorption of L1695 surfactant is related to the incorporation of sucrose diesters within the adsorption layer.

3.3. Properties of dynamic adsorption layers

The dynamic surface tensions were measured at three surfactant concentrations (0.01 wt%; 0.1 wt% and 1 wt%). Note that these concentrations are above CMC for both surfactants at $T \geq 40$ °C (see Fig. 2) with only 0.01 wt% being below CMC for L1695 without urea and for Brij L23 in the presence of urea. The measured dynamic surface tensions were used to calculate the dynamic adsorption as a function of universal surface age, t_u. It is calculated by dividing the nominal surface age by 37 [65]. The dynamic adsorption, $\Gamma(t)$ and the dynamic surface coverage, $\theta_{CMC}(t)$ are calculated using the following expressions [45]:

$$\Gamma(t) = \frac{1}{\alpha N_A} \frac{\frac{\pi_S(t)\alpha N_A}{RT}}{1 + \frac{\pi_S(t)\alpha N_A}{RT}} \tag{4}$$

$$\theta_{CMC}(t) = \frac{\Gamma(t)}{\Gamma_{CMC}} \tag{5}$$

where the dynamic surface pressure, $\pi_S(t)$, is related to the measured dynamic surface tension by $\pi_S(t) = \sigma_0 - \sigma(t)$.

The dependence of π_S *vs.* ln$t$ reveals three regions, see Figure S4. In the first region, observed only at low C_S and short t_u, the surface pressure $\pi_S \approx 0$, indicating minimal surfactant adsorption on the surface. This region persists up to $t_u = 10$ ms for 0.01 wt% L1695 and only to $t_u = 0.03$ ms for 0.01 wt% Brij L23. It is not observed at higher C_S as it ends even before the first experimental point can be reliably determined. In the second region, π_S increases linearly with ln$t$ with the increase is much steeper for L1695 compared to Brij L23 across all studied conditions. In the third region, a much slower increase of π_S *vs.* ln$t$ is observed. For Brij L23, the dynamic surface pressure almost reaches its equilibrium value, measured in the de Nouy ring experiment, while for L1695 solutions, especially at higher temperatures, a fourth region is observed in which π_S starts to increase further, see Figure S4 for example.

The first region is significantly shorter for Brij L23, indicating that the molecules adsorb very rapidly on the air-water interface, possibly due to the presence of molecules with smaller hydrophilic head. Consequently, at low C_S and shorter times, π_S for Brij L23 is higher compared to that for L1695. The steeper increase of π_S with ln$t$ for L1695 solutions, in the second region, leads to π_S being higher for L1695 in the third region as compared to Brij L23. To summarize, Brij L23 molecules adsorb faster on the interface, but cannot pack as well as L1695 molecules.

The presence of urea in L1695 solutions decreases the duration of the first region, and increases the slope in the second region, resulting in higher π_S of urea-containing solutions after 1000 ms. For Brij L23, urea increases the slope in the second region of the π_S *vs.* ln$t$ curve, without affecting the initial region.

The dynamic surface pressure, π_S at t_u= 10 ms at C_S = 0.1 wt%, is shown in Fig. 4 A and for all three studied surfactant concentrations in Figure S5 in SI. It is seen that $\pi_S(t_u = 10\text{ ms})$ is higher for Brij L23 compared to L1695 at all studied temperatures for C_S = 0.01 wt%, see Figure S5A. At this concentration, $t_u = 10$ ms is very close to the end of the first region for L1695, whereas it is in the second region for Brij L23: the shorter molecules in Brij L23 ensure faster adsorption at low C_s and short times. Increasing C_S to 0.1 wt% and 1 wt% leads to a significant increase in $\pi_S(t_u = 10\text{ ms})$ for L1695, and a smaller increase for Brij L23, as illustrated in Fig. 4 A and Figure S5B. At these concentrations, $\pi_S(t_u = 10\text{ ms})$ approaches the equilibrium surface pressure. The slower adsorption of L1695 at C_S = 0.01 wt% is, at least, partially related to the higher CMC values and its higher solubility. This is due to a greater number of H-bonds formed between its head group and the water molecules. At higher concentrations of L1695, the higher $\pi_S(t_u = 10\text{ ms})$ values are related to the formation of a denser adsorption layer, even under dynamic conditions. The effect of temperature on $\pi_S(t_u = 10\text{ ms})$ is relatively small for Brij L23, but noticeable for L1695 adsorption layers with a significant increase of $\pi_S(t_u = 10\text{ ms})$.

The measured values of π_S are used to determine the time dependence of Γ and θ_{CMC}, see Fig. 4B, S5 and S7. The increase of temperature increases significantly the dynamic adsorption $\Gamma(t_u = 10\text{ ms})$ for L1695 at all three concentrations studied, whereas $\Gamma(t_u = 10\text{ ms})$ slightly decreases for Brij L23. Regarding the effect of urea, it is similar to that of temperature: $\Gamma(t_u = 10\text{ ms})$ slightly decreases for Brij L23, and significantly increases for L1695 solutions.

The calculated dynamic surface coverage, θ_{CMC}, exhibits different behavior compared to the dynamic adsorption $\Gamma(t_u = 10\text{ ms})$, see Fig. 4 C. θ_{CMC} is higher for Brij L23 than for L1695 under all conditions studied, indicating faster kinetics of adsorption. Even after 10 ms, the characteristics of Brij L23 adsorption layers at $C_S \geq 0.1$ wt% are very similar to the characteristics of equilibrium adsorption layer. The increase of temperature leads to formation of adsorption layers closer to their equilibrium state for Brij L23, with θ_{CMC} approaching a value of 1. In contrast, the temperature rise decreases θ_{CMC} for L1695 solutions.

This surprising result could be explained as follows: at low temperatures, most of the diesters are unable to adsorb on the air-water interface and remain incorporated in the surfactant micelles. As a consequence, Γ_{CMC} is lower compared to that determined at higher temperatures, where some diesters adsorb on the air-water interface. At short time scales, a significant fraction of these diesters remain in the solution, leading to a decrease in θ_{CMC} upon increase of temperature. For 0.01 wt% L1695, the dynamic surface coverage remains low due to the slow adsorption of monoesters on the surface. The effect of urea on $\Gamma(t_u = 10\text{ ms})$ is similar to that of temperature: $\Gamma(t_u = 10\text{ ms})$ is higher for L1695 and lower for Brij L23, in accordance with the explanation for the changes in adsorption layer composition in the presence of urea.

In summary, the adsorption is faster for Brij L23 compared to L1695. For L1695, dynamic adsorption increases while dynamic surface coverage decreases with the increase of temperature, and with the addition of urea. This is explained by a higher amount of diesters, which control the surface properties of the equilibrium adsorption layers at high temperatures and in the presence of 6 M urea, but cannot adsorb rapidly under dynamic conditions. On the other hand, from Brij L23 solutions looser adsorption layers are formed at high temperatures, and in presence urea, which are easily reached.

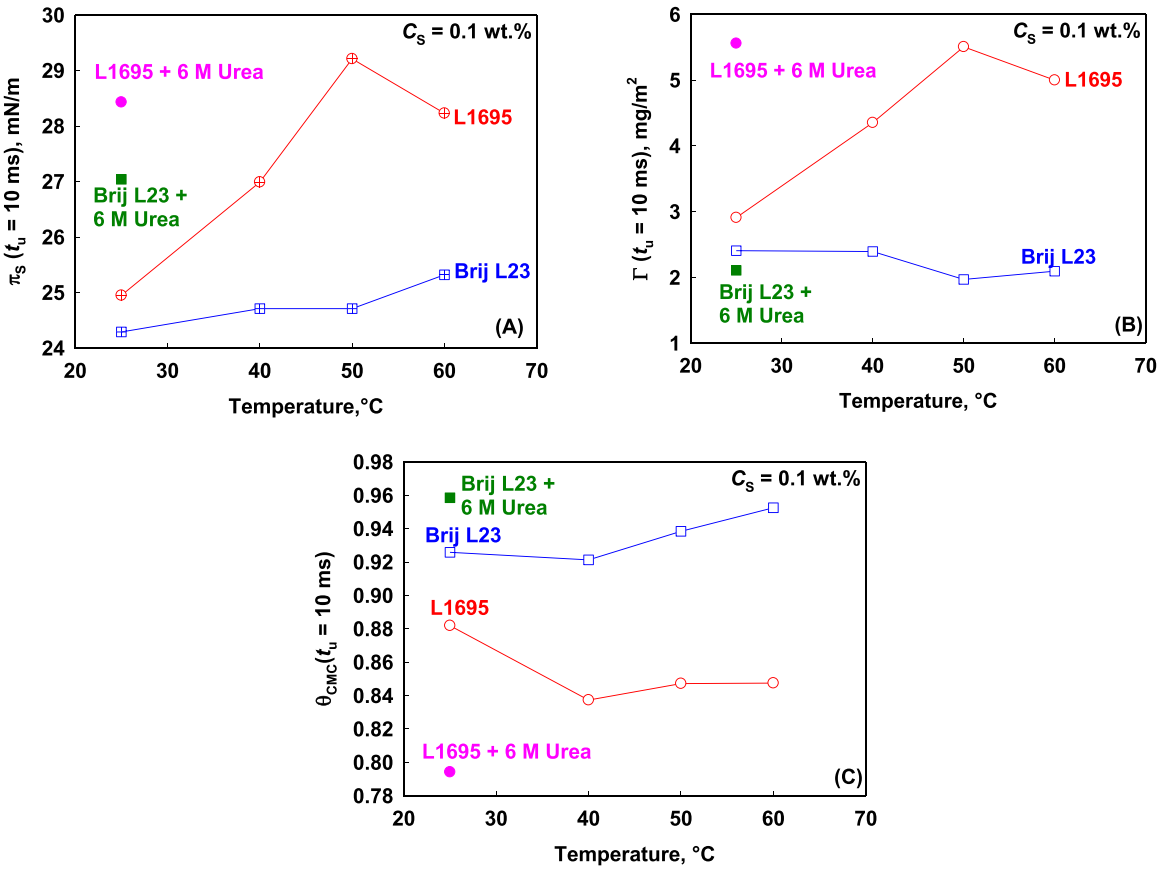

Fig. 4. (A) Dynamic surface pressure, π_S; (B) Dynamic surfactant adsorption, Γ; (C) Dynamic surface coverage, θ_{CMC} determined after 10 ms universal surface age as functions of temperature for Brij L23 (squares) and L1695 (circles) without (empty symbols) and with 6 M urea (full symbols) for 0.1 wt% surfactant solutions.

3.4. Foam film behavior

The behavior of foam films was investigated using 0.1 wt% and 1 wt % solutions of Brij L23 and L1695. Under all conditions, the observed film thinning was similar to the one typical for low molecular mass surfactants films, without indication for the formation of condensed adsorption layers on the film surfaces. The equilibrium film thickness was reached ≈ 1 min after film formation, during which a fast ejection of the entrapped dimples had occurred. Note that in presence of condense adsorption layer on the film surfaces, the rate of dimple ejection would be over 10 min [66]. Further film thinning was observed only for films formed from 1 wt% Brij L23, where a stepwise decrease in film thickness was observed. Films formed from 1 wt% Brij L23 at temperatures of 50 and 60°C ruptured after ca. 10 min after their formation. Illustrative

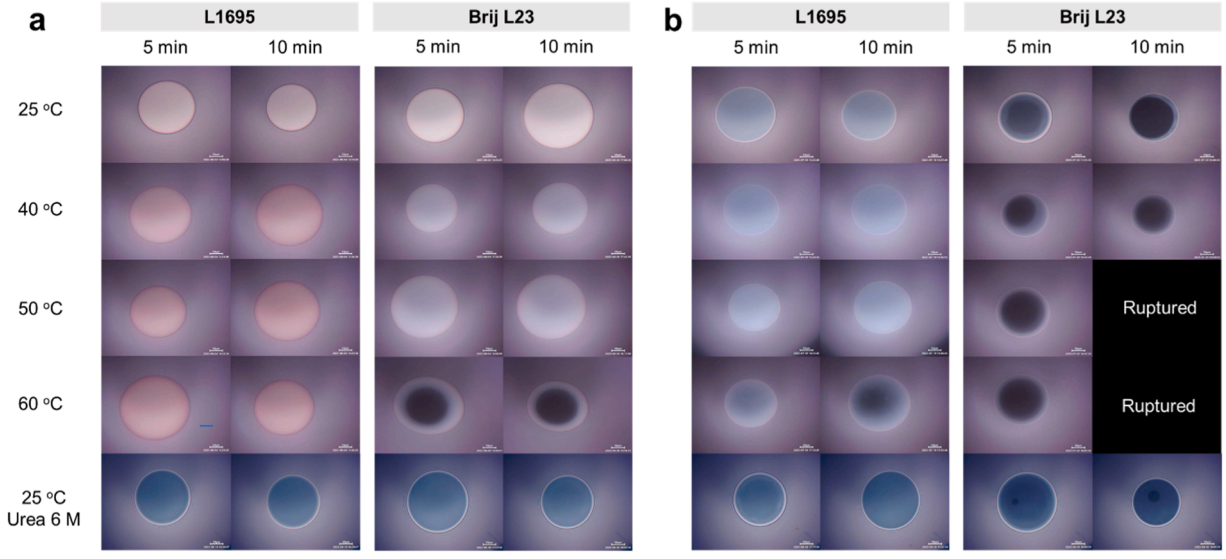

Fig. 5. Foam films formed from L1695 and Brij L23 (a) 0.1 wt% and (b) 1 wt% solutions, observed under polychromatic white light using an optical microscope at 25°C, 40°C, 50°C, 60°C, and at 25°C in 6 M urea solution. Pictures are taken 5 min and 10 min after the film formation.

images from these experiments are shown in Fig. 5.

The thickness of 0.1 wt% L1695 films was ≈ 100 nm and did not change significantly with temperature. Thinner films were formed from 1 wt% L1695 solution, with a thickness of about 70 nm. The addition of urea to 0.1 wt% and 1 wt% L1695 solutions further decreased the film thickness down to 50 nm. Regarding Brij L23, films with a thickness of about 90 nm were formed from 0.1 wt% solutions, and black spots with a thickness of about 20 nm were observed at $T = 60°C$. For 1 wt% Brij L23 solutions, black spots were observed at all temperatures. Upon addition of urea, the film thickness of 0.1 wt% Brij L23 decreased to 50 nm, whereas black spots of about 25 nm were observed for 1 wt% Brij L23 solution.

The formation of thick films from nonionic surfactants, such as alkyl glucoside surfactant, has been reported in the literature and was explained with the adsorption of hydroxyl (OH^-) ions on the film surfaces, inducing long-ranged electrostatic repulsion due to the low concentration of background electrolyte [67]. To confirm that this explanation stands for the thick films formed using L1695 in the current work, experiments were carried out with 10 mM sodium chloride (NaCl) solutions. A significant decrease in film thickness was observed, indicating that the observed thick films are related to the co-adsorption of surfactant molecules and OH^- ions. The thinner films, formed at higher surfactant concentration, are explained by the replacement of OH^- ions by surfactant molecules at the interface.

To investigate whether the film behavior in the presence of urea is related to suppression of the electrostatic repulsion, the conductivities of the solutions were measured. Values are provided in Table 1. The measured conductivities were significantly higher for solutions containing 6 M urea, suggesting the presence of ionic species in it. Those values were then used to estimate the ionic strength of the background electrolyte (see Table 1). The calculated values vary between 0.12 mM (0.1 wt% L1695) and 1.19 mM (1 wt% Brij L23 + urea). For calculation of the characteristic Debye length, κ^{-1}, dielectric constants of 78.3 for water and 94 for water-urea at 25 °C were used. The Debye length, κ^{-1}, varies between 9.7 nm (1 wt% Brij L23 + urea) and 27.7 nm (0.1 wt% L1695).

To assess the effect of electrostatic repulsion on the film behavior, the magnitudes of the electrostatic and van der Waals interactions were estimated using [57]:

$$\Pi = 64 n_0 k_B T \left[\tanh\left(\frac{e\Psi_s}{4k_B T}\right)\right]^2 \exp(-\kappa h) - \frac{A_H}{6\pi h^3} \quad (6)$$

where Π is the disjoining pressure acting between film surface, n_0 is the electrolyte number concentration, $k_B T$ is the thermal energy, κ is the inverse Debye screening length, Ψ_S is the electrical surface potential, e is the elementary charge, A_H is the Hamaker constant, and h is the film thickness. For Hamaker constant we used the values of 3.73×10^{-20} J for water solutions and 4.65×10^{-20} J for urea-water solutions, calculated using dielectric constants of 78.3 and 94, and refractive indexes of 1.333 and 1.38 for water and urea-water mixture, respectively.

Capillary pressures, P_C, leading to film thinning were calculated using the measured equilibrium surface tensions. The calculated values of P_C varied between 45 Pa and 67 Pa (see Table 1). The values of the surface potential for different systems were estimated from the equalization of the disjoining pressure, Π, calculated by Eq. (6) at the measured film thickness, and capillary pressures, P_C. The resulting $|\Psi_S|$ values, ranging from 14 mV to 36 mV, are within the range of values measured for xylene drops in the presence of different concentrations of $C_{16}EO_8$ [68]. The decrease in Ψ_S upon increasing the surfactant concentration is greater for Brij L23 compared to L1695. The estimated value of $|\Psi_S| = 14$ mV for 1 wt% Brij L23 predicts that the applied pressure will be enough to overcome the maximum in the electrostatic barrier, as observed experimentally (black spots in the center of the films). These thinner films are stabilized by a steric repulsion, explaining the destabilization of films formed at higher Brij L23 concentration and higher temperatures, as well as the lack of such effect at lower concentrations. Significant decrease in $|\Psi_S|$ is also observed for 0.1 wt% Brij L23 + urea solutions, but without black spot formation.

For L1695, a decrease in $|\Psi_S|$ is also observed upon increasing the concentration or addition of urea. However, the estimated value of $|\Psi_S|$, for 1 wt% L1695, is significantly higher compared to the one for Brij L23 (22 *vs.* 14 mV). This higher value of $|\Psi_S|$ for L1695 provides sufficient electrostatic repulsion (300 vs 67 Pa), preventing a transition to thinner steric-stabilized films at 25 °C. Under those conditions, the temperature increase up to 60°C further decreases the adsorbed OH^- ions on the interface. At this temperature, thinner films are observed after 10 min of storage (see Fig. 5), but they remain stable due to the increased surfactant adsorption, thus providing sufficient steric repulsion.

From this series of experiments, we conclude that there is a long-range electrostatic repulsion between the film surfaces at low surfactant concentrations. This repulsion decreases upon increasing the surfactant concentration due to the displacement of OH^- ions from the interface. Transition from electrostatically to sterically stabilized films with time is observed for 1 wt% Brij L23 stabilized films, under all studied conditions. Those sterically stabilized films are stable at 25°C and 40°C, and become unstable at temperatures of 50 °C and 60 °C, due to the lower surfactant adsorption. The urea decreases surface potential to a similar extent at lower concentrations of both surfactants. In 1 wt% Brij L23 solutions, surface potential is the lowest, and urea has no further decreasing effect on its value: films transition to sterically stabilized films in presence and in absence of urea.

Table 1
The measured electrical conductivity, λ, calculated ionic strength, I_S, under the assumption that the ionic species is NaCl (50.1 cm^2.S/mol for Na^+ and 76.4 cm^2.S/mol for Cl^-); Debye length, κ^{-1} at 25°C; capillary pressure, P_C, in the used cell for 250 μm diameter films; measured film thickness, h, before black spot formation; estimated surface potential, $|\Psi_S|$ and maximal disjoining pressure, Π_{MAX}.

System	λ, μS/cm	I_S, mM	κ^{-1}, nm	P_C, Pa	h, nm	$\|\Psi_S\|$, mV	Π_{MAX}, Pa
0.1 wt% L1695	15.7	0.12	27.7	54	100 ±10	36±7	800 ±300
1 wt% L1695	22.8	0.18	22.7	52	70±7	22±4	300 ±100
0.1 wt% L1695 + Urea	129.6	1.02	10.4	45	50±5	23±4	1100 ±500
1 wt% L1695 + Urea	143.2	1.13	9.9	45	50±5	25±5	1600 ±600
0.1 wt% Brij L23	16.4	0.13	26.7	67	92±8	35±6	800 ±300
1 wt% Brij L23	28.7	0.23	20.0	67	30±3	14±1	67±10
0.1 wt% Brij L23 + Urea	130.4	1.03	10.4	51	50±5	24±6	1300 ±800
1 wt% Brij L23 + Urea	150.1	1.19	9.7	51	35±4	15±2	200 ±100

3.5. Foam properties

The experimental data from the foaming experiments performed in Bartsch test are shown in Fig. 6. The foamability increases with the number of shaking cycles for 0.1 wt% and 1 wt% solutions, and remains very low for 0.01 wt% solutions for both surfactants. Significant difference in the foam volume is observed for 0.1 wt% surfactant, whereas it is very similar for the other two concentrations, see Fig. 6A.

Under all conditions, the foamability of 0.1 wt% L1695 solution is higher compared to that of Brij L23 solution. For both surfactants, the addition of urea decreases significantly the foamability of 0.1 wt% solutions. Regarding the effect of temperature, the foamability of Brij L23

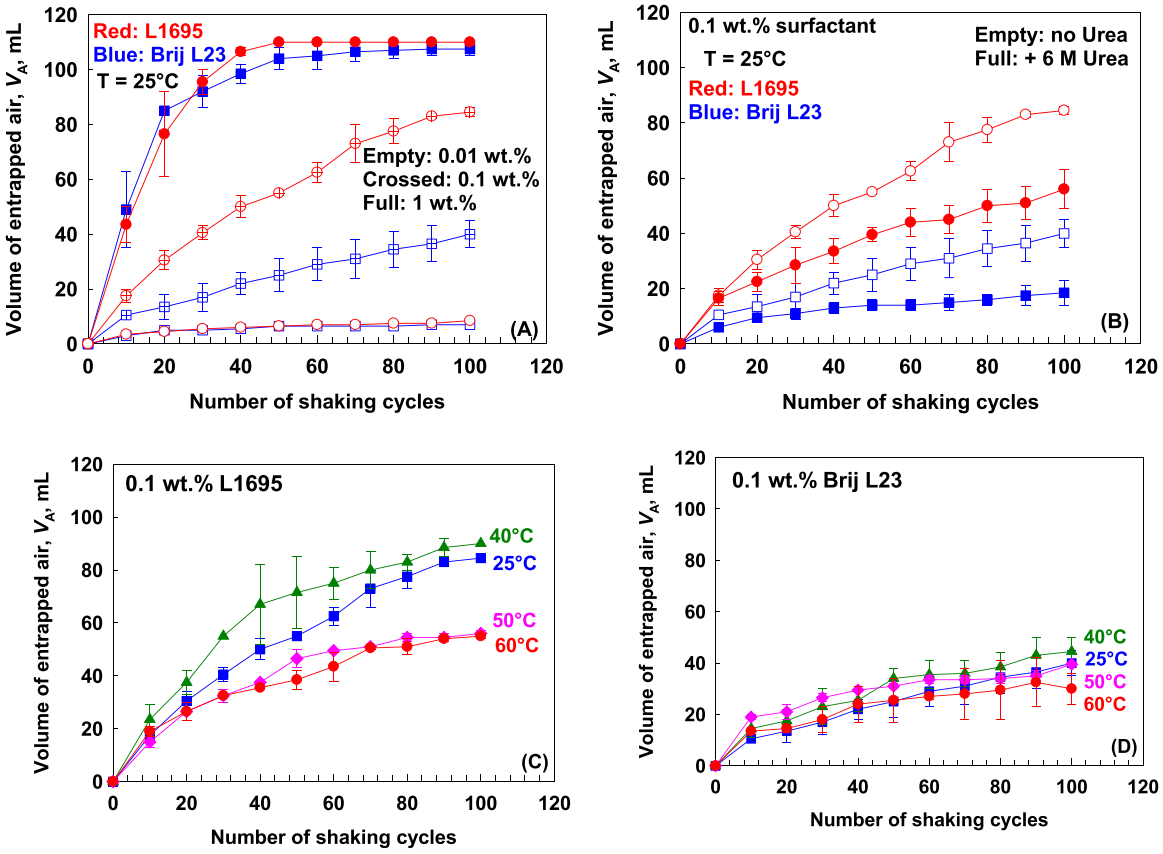

Fig. 6. Volume of entrapped air, V_A, in Bartsch test as a function of the number of shaking cycles for (A) L1695 (red symbols) and Brij L23 (blue symbols) solutions with concentrations, C_S, of 0.01 wt% (empty symbols); 0.1 wt% (crossed symbols); 1 wt% (full symbols) measured at 25°C; (B) 0.1 wt% surfactants without (empty symbols) and with 6 M urea (full symbols) measured at 25 °C; (C) 0.1 wt% L1695 and (D) 0.1 wt% Brij L23 at four different temperatures as indicated in the figure.

solution is little impacted, while in the case of 0.1 wt% L1695 it passes through a maximum at $T = 40$ °C, and decreases upon further increase of temperature to 50 and 60 °C. Changes in the temperature have no effect for the other two studied concentrations of L1695.

The experimental foamability results obtained in slow-foaming method FRM are shown in Fig. 7. One sees that temperature affects only the lowest studied concentration of 0.01 wt% for both surfactants. For this particular surfactant concentration, the increase of temperature leads to a higher foam volume. The same effect is also observed upon addition of urea – higher foamability is determined in 6 M urea, which is exactly the opposite of the trends observed in Bartsch test.

The evolution of the formed foams in both methods was monitored for 10 min after stopping the agitation. The foam volume as a function of time is shown in Fig. 8. The foams formed from L1695 solutions in Bartsch test remained stable at all studied temperatures in presence and in absence of urea, whereas significant bubble coalescence is observed in foams stabilized by Brij L23 solutions upon storage. The percentage of the air remaining in the foams after 10 min of storage is shown in Fig. 9 as a function of temperature for $C_S = 1$ wt%. It is seen that L1695 foams, with and without urea, remain stable, whereas the stability of Brij L23 foams decrease with increase of temperature from 75% at 25 °C down to 5 % at 60 °C. The addition of urea to Brij L23 stabilized foams leads to a

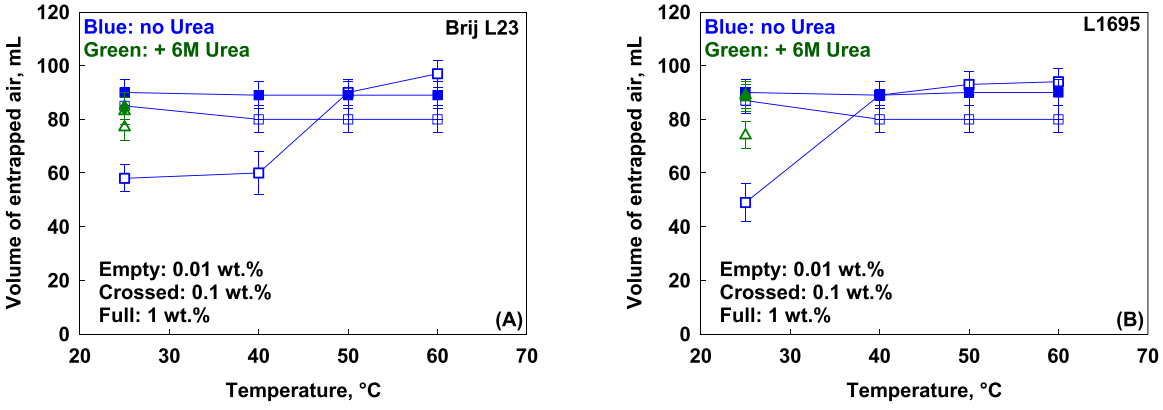

Fig. 7. Volume of entrapped air, V_A, in the bubbling method, as a function of temperature T for (A) Brij L23 and (B) L1695 solutions with concentrations of 0.01 wt% (empty symbols); 0.1 wt% (crossed symbols); 1 wt% (full symbols) without (blue symbols) and with 6 M urea (green symbols) after 15 s of air sparging in 20 mL surfactant solution.

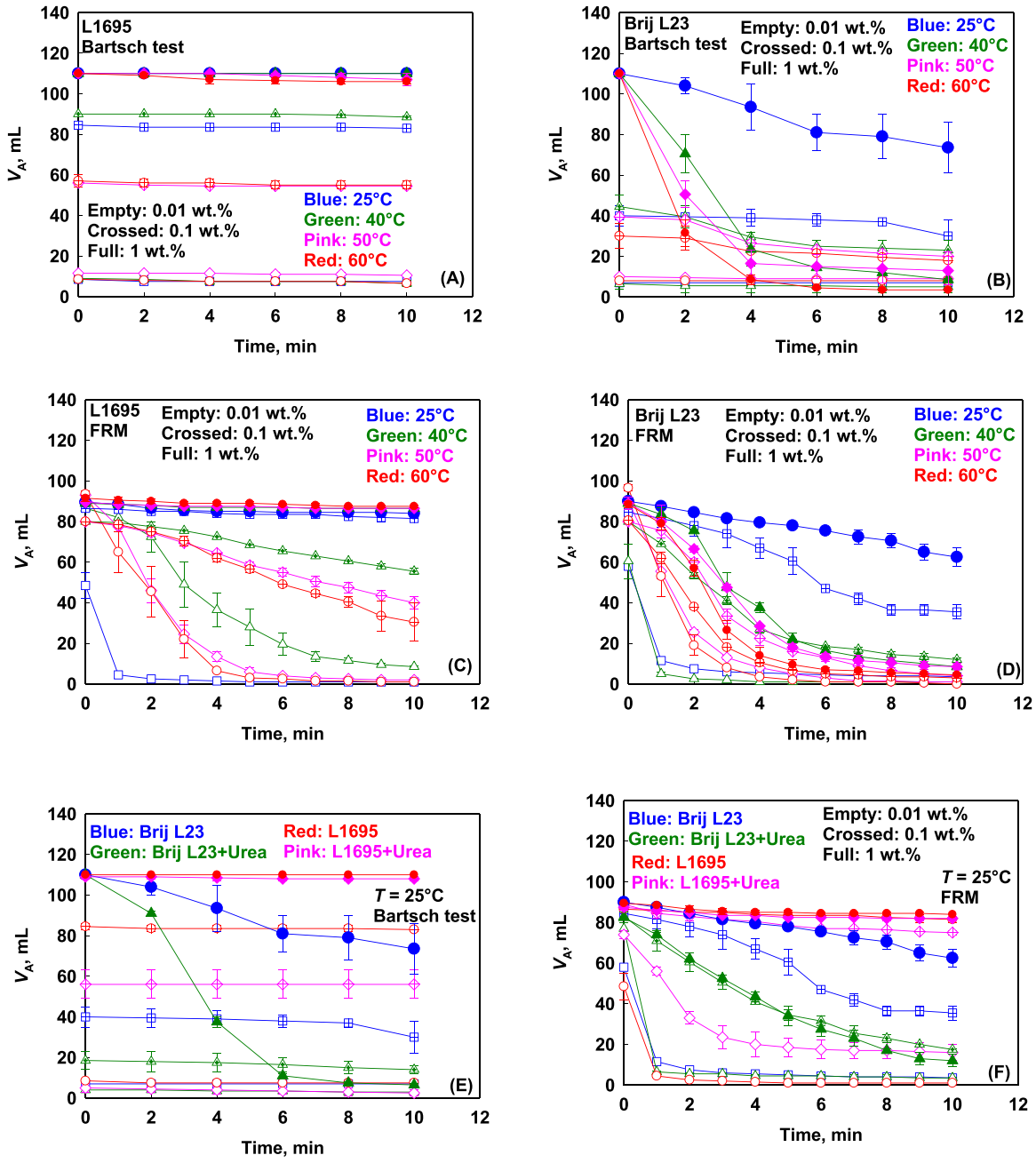

Fig. 8. Evolution of entrapped air volume, V_A, over 10 min for foams formed in (A, C, E) Brij L23 and (B, D, F) L1695 solutions in (A, B, E) Bartsch test, BT, and (C, D, F) bubbling method, FRM, from solutions with concentrations of 0.01 wt% (empty symbols); 0.1 wt% (crossed symbols); 1 wt% (full symbols) at (A, B, C, D) four different temperatures without urea, and at 25°C with and without urea (E, F).

significant decrease of foam stability, reaching the typical value for foams stored at high temperature.

From this series of experiments, it appears that the foamability increases significantly with the surfactant concentration from 0.01 wt% to 1 wt% in BT, whereas much smaller increase is observed for foams formed in FRM in the same concentration range. The temperature and presence of urea only affect the foamability for concentrations around the threshold concentration, required to reach the maximal foamability in a given foaming test, *i.e.*, ≈ 0.1 wt% for BT and ≈ 0.01 wt% for FRM. In BT, the foamability of 0.1 wt% L1695 passes through a maximum at T = 40 °C, whereas it decreases for 0.1 wt% L1695 and Brij L23 in the presence of urea.

In our previous studies [45,46], it was shown that the foamability depends on the dynamic surface coverage, and the type of forces acting between the foam film surfaces. Two well-distinguished curves for ionic and nonionic surfactants were found to describe the experimental data, obtained with a wide range of surfactants. In these previous studies [45–47], all experiments were performed at room temperature, and good correlation between the foamability and the dynamic surface tension was established.

In the current study, we performed experiments at different temperatures, and the experimental data for V_A *vs.* dynamic surface tension are compared with the previously obtained data, see Figure S10 in SI. To yield an air entrapment $V_A \geq 20$ mL in the BT method, the threshold dynamic surface tension was found to be ≈ 50 mN/m at room temperature [45,46]. However, decreasing the dynamic surface tension down to 50 mN/m is not sufficient to ensure foam generation from Brij L23 and L1695 solutions at higher temperatures, see Figure S10 in SI. This

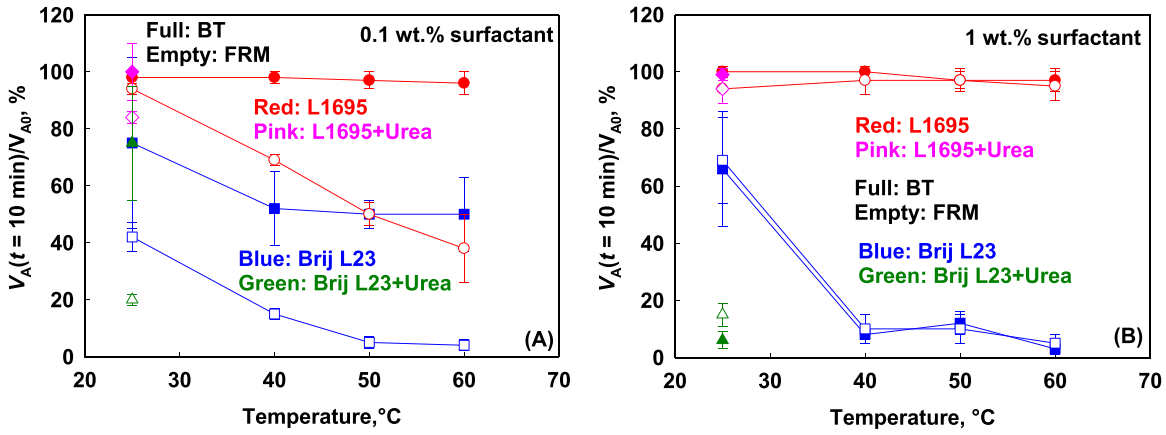

Fig. 9. Percentage of remaining foam 10 min after stopping the agitation, $V_A(t{=}10\ min)/V_{A0}$, for foams, generated in Bartsch test (BT, full symbols) and in bubbling method (FRM, empty symbols) from (A) 0.1 wt% and (B) 1 wt% solutions of L1695 (red circles); L1695 + 6 M urea (pink diamonds); Brij L23 (blue squares) and Brij L23+6 M urea (green triangles).

clearly shows that dynamic surface tension per se is not the key factor for the foamability of nonionic surfactants. Therefore, the data shown in Figure S10 were replotted as a function of the dynamic surface pressure, which is directly related to the dynamic adsorption, to determine whether it is the key factor for foamability, see Figure S11 in SI. The results at different temperatures match much better the results shown in Ref. [45], even though some slight deviation remains. Note that higher dynamic surface pressures are required at higher temperature to increase the foamability of the solutions.

Fig. 10 shows the relative foamability as a function of the dynamic surface coverage, θ_{CMC}. One sees that the data from the current study, *i.e.*, Brij L23 and L1695 foams at four different temperature and for the two different foaming methods, lay between the curves for Brij 58 and Brij 35 (dashed curve) and Tween 20 (dash-dot curve) foams formed at 25°C in three different methods [46]. The difference between Tween 20, on one side, and Brij 58 and Brij 35, on the other side, was explained in Ref. [46] with the occurrence of weak electrostatic repulsion in Tween 20. Here, similar explanation accounts for the lower threshold θ_{CMC}, required for increasing the foamability of the studied solutions. The

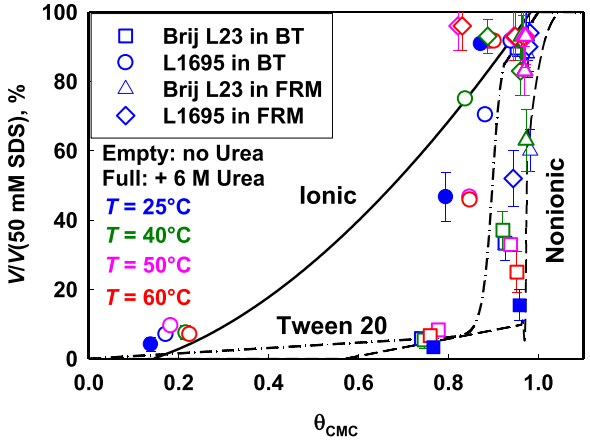

Fig. 10. Relative foamability, compared to that of 50 mM sodium dodecyl sulfate (SDS), V/V(50 mM SDS), as a function of the surface coverage, θ_{CMC}, for Brij L23 and L1695 foams, formed in Bartsch test (BT) and foam rise method (FRM) at different temperatures, with and without urea. The curves representing the dependence of the relative foamability with the surface coverage for foams formed at 25°C in different methods, are taken from Ref. [46] for ionic surfactants (continuous curve); nonionic Tween 20 (dash-dot curve) and for nonionic Brij 35 and Brij 58 (dashed curve). θ_{CMC} is determined using dynamic surface tension values after t_u = 10 ms for BT (measured by MBPM), and after 50 s for the FRM (measured by Wilhelmy plate method).

electrostatic repulsion is stronger for L1695 solutions, compared to Brij L23 and, as a consequence, the critical θ_{CMC} for reaching 50% of maximal foamability is lower for L1695 ($\theta_{CMC} \approx 0.8$) compared to Brij L23 ($\theta_{CMC} \approx 0.95$). This result agrees well with the estimated higher surface potentials for 1 wt% L1695 solutions, see Table 1. Those results indicate that long-range repulsion between the foam film surfaces decreases the critical θ_{CMC} value for nonionic surfactants required to reach substantial foam volume. Note that similar effect was determined for PVA solutions: long-range steric repulsion decreases the threshold surface coverage to 80% [47] as it is observed here for L1695 solutions.

The effect of urea on Brij L23 foams falls within the same explanation: it decreases long-range repulsions by replacing the hydroxyl anions from the interface. As a consequence, the threshold θ_{CMC} value reaches 95%, which is the typical value for nonionic surfactants without electrostatic or steric repulsion. However, the effect of urea on L1695 foams differs: it does not decrease the surface potential for 1 wt% L1695, see Table 1, and the weak electrostatic repulsion remains. Consequently, the threshold θ_{CMC} value for L1695 in the presence of urea is even lower, compared to solutions without urea: both the weak electrostatic repulsion and the higher adsorption decrease the probability for film rupture during the foaming process.

Therefore, it can be concluded that the approach, developed in Ref. [45,46] can be also used to account for the foamability differences observed with temperature, and in presence of urea. The weak electrostatic repulsion, arising from the adsorption of OH^- ions on the bubble surfaces, has noticeable beneficial effect for L1695 foamability, compared to Brij L23.

The foam stability depends significantly on the surfactant type and its concentration, but also on the method used for foam generation, the temperature and the presence of urea. As a rule, L1695 foams are more stable compared to Brij L23 ones. The longer stability of L1695 foams is related to the formation of denser adsorption layers on the bubble surfaces, as shown from the surface tension measurements. This is due to the presence of diesters in the surfactant. Along with the higher adsorption, the films formed from L1695 solutions exhibit a weak long-range electrostatic repulsion which also contributes towards the increased foam stability. The temperature increase does not affect the stability of L1695 foams formed in BT, regardless of the concentration. However, the foam stability decreases with T for foams prepared by FRM at the lowest surfactant concentrations (0.01 wt% and 0.1 wt%), see Fig. 9.

The significant stability difference between the foams generated in BT and in FRM at low concentrations (0.1 wt% and 0.01 wt%) is related to the bubble size. Bigger bubbles are formed in the FRM during gas blowing, whereas such big bubbles coalesce in BT, and only small bubbles remain at the end of the foam generation period, see Fig. 11. It is

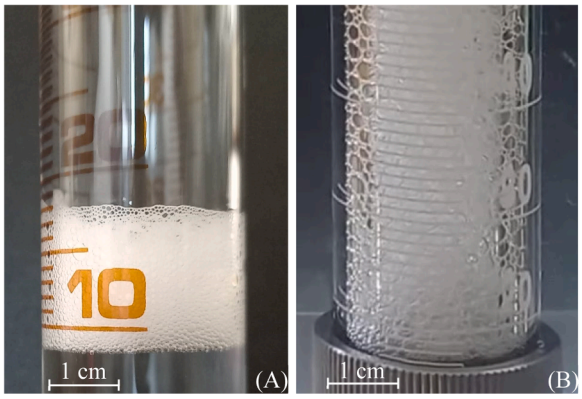

Fig. 11. Pictures taken immediately after the generation of foams has stopped. The foams are prepared from 0.01 wt% L1695 solutions at T = 60 °C in (A) Bartsch test and (B) foam rise method.

well known from the literature that the bigger the films, the less stable they are [69]. As a consequence, the stability of foams formed in FRM, is lower compared to the foams formed in BT. Increasing the L1695 concentration does not significantly impact the bubble size in FRM, but it does improve the stability. This is related to the formation of denser adsorption layers at higher surfactant concentrations, which is well seen from the Wilhelmy plate measurements, see Figure S12 in SI. Note that in our previous study, we showed that the Wilhelmy plate method is the relevant technique for assessing the surface properties of adsorption layers, formed on the bubble surfaces, produced in FRM [46]. The fact that both 0.1 wt% and 1 wt% L1695 solutions have identical surface tension at 25°C, is also in good agreement with their very good foam stability at 25 °C. Therefore, it can be concluded that the stabilization of big bubbles requires a surface coverage above 95%, even for L1695. The addition of urea has no significant impact on the stability of foams, formed from L1695 solutions, in good agreement with the high adsorptions, measured for this surfactant.

The stability of Brij L23 foams decreases with the increase of temperature in both methods. However, this is not related to variations in bubble size, because the foams formed in BT at different temperatures have very similar bubble size distributions, see Figure S13. The observed decreased stability is related to the lower adsorption of Brij L23 at higher temperature, decreased electrostatic repulsion and higher lateral attraction within the adsorption layer. This facilitates the formation of surfactant aggregates and bare surface in the film (weak spot), increasing the probability for film rupture. The presence of 6 M Urea in the solution decreases significantly the foam stability, in agreement with the lower adsorption.

From this discussion, it can be concluded that several important factors must be considered for foam stability after stopping the agitation: (1) The bubble size – foams containing bigger bubbles are less stable; (2) Temperature - higher temperature promotes foam destabilization for loosely packed adsorption layers, such as Brij L23, by increasing the probability for formation of surfactant-depleted zones and film breakage. Even in densely packed adsorption layers such as those of L1695, temperature elevates the probability of foam destruction in foams with large bubbles. However, if the surfactant concentration is high enough to ensure fast adsorption, those foams remain stable; (3) Urea - the addition of urea, replacing water molecules from the hydration shell of Brij L23, decreases the foam stability due to weaker steric repulsion between surfactant head groups, increasing the probability of weak spots formation inside the adsorption layer. The addition of urea does not have any effect on L1695 foams stability: it is unable to replace

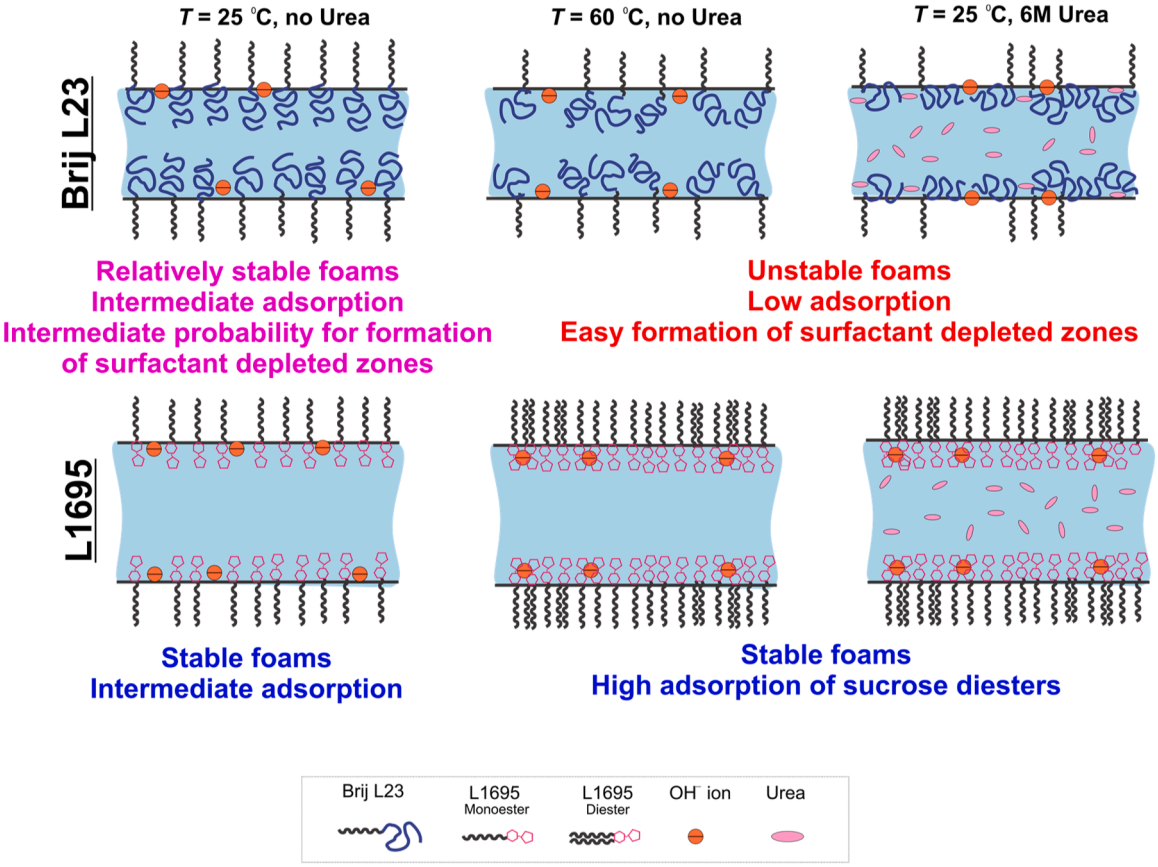

Fig. 12. Schematic representation of the films formed between two neighboring bubbles in Brij L23 and L1695 foams formed either at 25 and 60°C without urea, and at 25°C in presence of urea.

the water molecules around the sugar head groups, thus leading to higher adsorption of these molecules on the air-water interface.

A comparative schematic representation of L1695 and Brij L23 foam films stability under different conditions is shown in Fig. 12.

4. Conclusions

Systematic series of experiments with two C12 nonionic surfactants, namely Brij L23 and L1695, were performed to compare their surface, film and foam properties at temperatures ranging between 25 and 60°C. Additional experiments at 25°C with 6 M Urea were conducted to examine the impact of H-bonding.

The temperature increase leads to lower adsorption on air-water interface without changing the micelles formed in the solution for Brij L23 surfactant. In contrast, a significant increase of surfactant adsorption, attributed to the presence of diesters that incorporate faster into the adsorption layer at higher temperatures, is determined for L1695 surfactant.

The addition of 6 M urea had opposite effects on the two surfactants. For Brij L23, it increased CMC and decreased adsorption, as the urea molecules replaced water in the hydration shell, weakening the hydrophobic interactions between surfactant tails. Conversely, in L1695 solutions, urea strengthened the hydrophobic interactions between surfactant tails because it is unable to intercalate between the surfactant head groups and stays in bulk water, leading to decreased CMC and increased adsorption. To the best of our knowledge this is the first study in which the decrease of CMC is reported upon addition of 6 M urea in the surfactant solution.

At low surfactant concentrations, the adsorption of the hydroxyl anion on the air-water interface resulted in the formation of thick foam films for both surfactants. Increasing temperature significantly reduced the film thickness for Brij L23, while the L1695 stabilized films remained thick even at higher surfactant concentrations and at higher temperatures.

The observed foamability trends were consistent with those seen for nonionic surfactants exhibiting weak electrostatic repulsion [46]. Temperature increase led to reduced electrostatic repulsion for Brij L23, raising the threshold surface coverage for good foamability ($\theta_{CMC} \approx 0.95$). For L1695, an increased surfactant adsorption, and the electrostatic repulsion being maintained at higher temperatures, allowed formation of voluminous foam at lower surface coverage of $\theta_{CMC} \approx 0.8$.

Brij L23 foam stability decreased with temperature, due to the lower surfactant adsorption and increased attraction between the surfactant molecules within the adsorption layer, thus leading to bare spots on the film surfaces. L1695 foam stability remained unaffected by temperature in both Bartsch and foam rise tests at higher surfactant concentration, whereas the formed big bubbles in foams generated in FRM at lower concentrations leads to destabilization of foams at higher temperature.

This study demonstrates the applicability of the previously developed approach for analyzing the foamability at room temperature [45, 46] to foams formed at higher temperatures. The correlation between the relative foamability and dynamic surface coverage, rather than the dependence on dynamic surface tension, is needed to explain the observed trends. Potential limitations of the developed approach could be met in the case of non-Newtonian behavior of the foaming solutions. Further investigations are currently being carried out on this topic.

The stability of the formed foams is strongly temperature-dependent only when the temperature rise leads to lower surfactant adsorption, as observed for Brij L23, whereas it remains unaffected when the adsorption increases with temperature as in the case of L1695. These findings suggest potential applications of surfactant mixtures, particularly sucrose mono- and diesters, in various industries utilizing foams. Further studies could expand and deepen this approach across different foam tests and surfactant systems.

Funding

This study is financed by the European Union-Next Generation EU, through the National Recovery and Resilience Plan of the Republic of Bulgaria, project N° BG-RRP-2.004-0008-C01.

CRediT authorship contribution statement

Lucie Delforce: Writing – original draft, Validation, Investigation, Formal analysis, Data curation. **Slavka Tcholakova:** Writing – review & editing, Visualization, Validation, Supervision, Methodology, Funding acquisition, Formal analysis, Conceptualization.

Declaration of Competing Interest

The authors declare that they have no known competing financial interests or personal relationships that could have appeared to influence the work reported in this paper

Data Availability

Data will be made available on request.

Acknowledgment

The authors thank Mrs. Nevena Pagureva, Mr. Vassil Georgiev, Mrs. Dora Dimitrova and Mr. Vladimir Petkov, all from Sofia University, for their help for experiments. We are grateful to Prof. Nikolai Denkov (Sofia University) and Dr. Diana Cholakova (Sofia University) for the insightful discussions and for the critical reading of the manuscript.

Appendix A. Supporting information

Supplementary data associated with this article can be found in the online version at doi:10.1016/j.colsurfa.2024.133844.

References

[1] N.S. Neta, J.A. Teixeira, L.R. Rodrigues, Sugar ester surfactants: enzymatic synthesis and applications in food industry, Crit. Rev. Food Sci. Nutr. 55 (2015) 595–610, https://doi.org/10.1080/10408398.2012.667461.
[2] I. Kralova, J. Sjöblom, Surfactants used in food industry: a review, J. Dispers. Sci. Technol. 30 (2009) 1363–1383, https://doi.org/10.1080/01932690902735561.
[3] H. Zhang, F. Feng, J. Li, X. Zhan, H. Wei, H. Li, H. Wang, X. Zheng, Formulation of food-grade microemulsions with glycerol monolaurate: effects of short-chain alcohols, polyols, salts and nonionic surfactants, Eur. Food Res. Technol. 226 (2008) 613–619, https://doi.org/10.1007/s00217-007-0606-z.
[4] K. Hill, O. Rhode, Sugar-based surfactants for consumer products and technical applications, Lipid / Fett 101 (1999) 25–33, https://doi.org/10.1002/(SICI)1521-4133(19991)101:1<25::AID-LIPI25>3.0.CO;2-N.
[5] S. Chen, S. Hanning, J. Falconer, M. Locke, J. Wen, Recent advances in non-ionic surfactant vesicles (niosomes): fabrication, characterization, pharmaceutical and cosmetic applications, Eur. J. Pharm. Biopharm. 144 (2019) 18–39, https://doi.org/10.1016/j.ejpb.2019.08.015.
[6] T. Tamura, Y. Kaneko, M. Ohyama, Dynamic surface tension and foaming properties of aqueous polyoxyethylene n-dodecyl ether solutions, J. Colloid Interface Sci. 173 (1995) 493–499, https://doi.org/10.1006/jcis.1995.1351.
[7] S. Yada, T. Suzuki, S. Hashimoto, T. Yoshimura, Adsorption and aggregation properties of homogeneous polyoxypropylene–polyoxyethylene alkyl ether type nonionic surfactants, Langmuir 33 (2017) 3794–3801, https://doi.org/10.1021/acs.langmuir.7b00104.
[8] D.J. Mitchell, G.J.T. Tiddy, L. Waring, T. Bostock, M.P. McDonald, Phase behaviour of polyoxyethylene surfactants with water. Mesophase structures and partial miscibility (cloud points), J. Chem. Soc., Faraday Trans. 1 79 (1983) 975–1000, https://doi.org/10.1039/F19837900975.
[9] L.-J. Chen, S.-Y. Lin, C.-C. Huang, E.-M. Chen, Temperature dependence of critical micelle concentration of polyoxyethylenated non-ionic surfactants, Colloids Surf. A Physicochem. Eng. Asp. 135 (1998) 175–181, https://doi.org/10.1016/S0927-7757(97)00238-0.
[10] Z.-L. Chen, Y.-L. Yan, X.-B. Huang, Stabilization of foams solely with polyoxyethylene-type nonionic surfactant, Colloids Surf. A Physicochem. Eng. Asp. 331 (2008) 239–244, https://doi.org/10.1016/j.colsurfa.2008.08.011.
[11] F. Mustan, N. Politova-Brinkova, Z. Vinarov, D. Rossetti, P. Rayment, S. Tcholakova, Interplay between bulk aggregates, surface properties and foam

stability of nonionic surfactants, Adv. Colloid Interface Sci. 302 (2022) 102618, https://doi.org/10.1016/j.cis.2022.102618.
[12] A. Berthod, S. Tomer, J.G. Dorsey, Polyoxyethylene alkyl ether nonionic surfactants: physicochemical properties and use for cholesterol determination in food, Talanta 55 (2001) 69–83, https://doi.org/10.1016/S0039-9140(01)00395-2.
[13] B.A.P. Nelen, L. Bax, J.M. Cooper, Sucrose Esters. Emulsifiers in Food Technology, John Wiley & Sons, Ltd, 2014, pp. 147–180, https://doi.org/10.1002/9781118921265.ch7.
[14] G. Garofalakis, B.S. Murray, Dilatational rheology and foaming properties of sucrose monoesters in the presence of β-lactoglobulin, Colloids Surf. B 21 (2001) 3–17, https://doi.org/10.1016/S0927-7765(01)00179-5.
[15] Y. Liu, B.P. Binks, A novel strategy to fabricate stable oil foams with sucrose ester surfactant, J. Colloid Interface Sci. 594 (2021) 204–216, https://doi.org/10.1016/j.jcis.2021.03.021.
[16] F.A. Husband, D.B. Sarney, M.J. Barnard, P.J. Wilde, Comparison of foaming and interfacial properties of pure sucrose monolaurates, dilaurate and commercial preparations, Food Hydrocoll. 12 (1998) 237–244, https://doi.org/10.1016/S0268-005X(98)00036-8.
[17] S.E.H.J. Van Kempen, H.A. Schols, E. Van Der Linden, L.M.C. Sagis, Effect of variations in the fatty acid chain of oligofructose fatty acid esters on their foaming functionality, Food Biophys. (2013), https://doi.org/10.1007/s11483-013-9324-1.
[18] F. Sterpone, C. Pierleoni, G. Briganti, M. Marchi, Structure and dynamics of hydrogen bonds in the interface of a C12E6 Spherical Micelle in water solution: a md study at various temperatures, J. Phys. Chem. B 110 (2006) 18254–18261, https://doi.org/10.1021/jp0602070.
[19] V.S. Marinov, H. Matsuura, Raman spectroscopic study of temperature dependence of water structure in aqueous solutions of a poly(oxyethylene) surfactant, J. Mol. Struct. 610 (2002) 105–112, https://doi.org/10.1016/S0022-2860(02)00023-6.
[20] L.S. Romsted, J. Yao, Arenediazonium Salts: new probes of the interfacial compositions of association colloids. 4.[1–3] estimation of the hydration numbers of aqueous hexaethylene glycol monododecyl Ether, $C_{12}E_6$, micelles by chemical trapping, Langmuir 12 (1996) 2425–2432, https://doi.org/10.1021/la950737f.
[21] H. Wang, W. Guo, C. Zheng, D. Wang, H. Zhan, Effect of temperature on foaming ability and foam stability of typical surfactants used for foaming agent, J. Surfactants Deterg. 20 (2017) 615–622, https://doi.org/10.1007/s11743-017-1953-9.
[22] A. Rezaei, Z. Derikvand, R. Parsaei, M. Imanivarnosfaderani, Surfactant-silica nanoparticle stabilized N_2-foam flooding: a mechanistic study on the effect of surfactant type and temperature, J. Mol. Liq. 325 (2021) 115091, https://doi.org/10.1016/j.molliq.2020.115091.
[23] K. Oetjen, C. Bilke-Krause, M. Madani, T. Willers, Temperature effect on foamability, foam stability, and foam structure of milk, Colloids Surf. A Physicochem. Eng. Asp. 460 (2014) 280–285, https://doi.org/10.1016/j.colsurfa.2014.01.086.
[24] M. Kanduč, E. Schneck, C. Stubenrauch, Intersurfactant H-Bonds between head groups of n-dodecyl-β-D-maltoside at the air-water interface, J. Colloid Interface Sci. 586 (2021) 588–595, https://doi.org/10.1016/j.jcis.2020.10.125.
[25] D. Ranieri, N. Preisig, C. Stubenrauch, On the influence of intersurfactant H-bonds on foam stability: a study with technical grade surfactants, Tenside Surfactants Deterg. 55 (2018) 6–16, https://doi.org/10.3139/113.110537.
[26] K. Schellmann, N. Preisig, P. Claesson, C. Stubenrauch, Effects of protonation on foaming properties of dodecyldimethylamine oxide solutions: a pH-study, Soft Matter 11 (2015) 561–571, https://doi.org/10.1039/C4SM02476A.
[27] C. Stubenrauch, M. Hamann, N. Preisig, V. Chauhan, R. Bordes, On how hydrogen bonds affect foam stability, Adv. Colloid Interface Sci. 247 (2017) 435–443, https://doi.org/10.1016/j.cis.2017.02.002.
[28] N. Preisig, T. Schad, L. Jacomine, R. Bordes, C. Stubenrauch, How promoting and breaking intersurfactant h-bonds impact foam stability, Langmuir 35 (2019) 14999–15008, https://doi.org/10.1021/acs.langmuir.9b02407.
[29] N. Raykundaliya, R. Bordes, K. Holmberg, J. Wu, P. Somasundaran, D.O. Shah, The effect on solution properties of replacing a hydrogen atom with a methyl group in a surfactant, Tenside Surfactants Deterg. 52 (2015) 369–374, https://doi.org/10.3139/113.110387.
[30] J.R. Kanicky, A.F. Poniatowski, N.R. Mehta, D.O. Shah, Cooperativity among molecules at interfaces in relation to various technological processes: effect of chain length on the pka of fatty acid salt solutions, Langmuir 16 (2000) 172–177, https://doi.org/10.1021/la990719o.
[31] J. Boos, W. Drenckhan, C. Stubenrauch, Protocol for studying aqueous foams stabilized by surfactant mixtures, J. Surfact. Deterg. 16 (2013) 1–12, https://doi.org/10.1007/s11743-012-1416-2.
[32] S. Tsibranska, A. Ivanova, S. Tcholakova, N. Denkov, Structure and undulations of escin adsorption layer at water surface studied by molecular dynamics, Molecules 26 (2021) 6856, https://doi.org/10.3390/molecules26226856.
[33] S. Tsibranska, A. Ivanova, S. Tcholakova, N. Denkov, Structure of dense adsorption layers of escin at the air–water interface studied by molecular dynamics simulations, Langmuir 35 (2019) 12876–12887, https://doi.org/10.1021/acs.langmuir.9b02260.
[34] N. Pagureva, S. Tcholakova, K. Golemanov, N. Denkov, E. Pelan, S.D. Stoyanov, Surface properties of adsorption layers formed from triterpenoid and steroid saponins, Colloids Surf. A Physicochem. Eng. Asp. 491 (2016) 18–28, https://doi.org/10.1016/j.colsurfa.2015.12.001.
[35] K. Golemanov, S. Tcholakova, N. Denkov, E. Pelan, S.D. Stoyanov, Remarkably high surface visco-elasticity of adsorption layers of triterpenoid saponins, Soft Matter 9 (2013) 5738, https://doi.org/10.1039/c3sm27950b.
[36] L. Delforce, V. Nardello-Rataj, R. Lebeuf, J.-M. Aubry, J.F. Ontiveros, Self-aggregation, dilational surface rheology and foaming properties of 1-O-dodecyl diglyceryl ether compared to n-dodecyl-β-D-maltoside and pentaethyleneglycol monododecyl ether, J. Mol. Liq. 388 (2023) 122795, https://doi.org/10.1016/j.molliq.2023.122795.
[37] S. Tcholakova, F. Mustan, N. Pagureva, K. Golemanov, N.D. Denkov, E.G. Pelan, S. D. Stoyanov, Role of surface properties for the kinetics of bubble Ostwald ripening in saponin-stabilized foams, Colloids Surf. A Physicochem. Eng. Asp. 534 (2017) 16–25, https://doi.org/10.1016/j.colsurfa.2017.04.055.
[38] P.K. Das Gupta, S.P. Moulik, Effects of urea and a nonionic surfactant on the micellization and counterion binding properties of cetyltrimethyl ammonium bromide and sodium dodecyl sulfate, Colloid Polym. Sci. 267 (1989) 246–254, https://doi.org/10.1007/BF01410582.
[39] M.J. Schick, Effect of electrolyte and urea on micelle formation[1], J. Phys. Chem. 68 (1964) 3585–3592, https://doi.org/10.1021/j100794a025.
[40] L. Costantino, G. D'Errico, P. Roscigno, V. Vitagliano, Effect of urea and alkylureas on micelle formation by a nonionic surfactant with short hydrophobic tail at 25 °C, J. Phys. Chem. B 104 (2000) 7326–7333, https://doi.org/10.1021/jp0012808.
[41] G. Briganti, S. Puvvada, D. Blankschtein, Effect of urea on micellar properties of aqueous solutions of nonionic surfactants, J. Phys. Chem. 95 (1991) 8989–8995, https://doi.org/10.1021/j100175a103.
[42] C.L. Bianco, C.S. Schneider, M. Santonicola, A.M. Lenhoff, E.W. Kaler, Effects of urea on the microstructure and phase behavior of aqueous solutions of poly (oxyethylene) surfactants, Ind. Eng. Chem. Res. 50 (2011) 85–96, https://doi.org/10.1021/ie101011v.
[43] J.A. Schellman, C. Schellman, The conformation of polypeptide chains in proteins, in: H. Neurath (Ed.), The Proteins Composition, Structure, and Function, Second ed., Academic Press, New York, 1964, pp. 1–137, https://doi.org/10.1016/B978-0-12-395724-5.50011-9.
[44] H. Schott, Effect of electrolytes on foaming of nonionic surfactant solutions, JAOCS 65 (1988) 1658–1663, https://doi.org/10.1007/BF02912572.
[45] B. Petkova, M. Chenkova, K. Golemanov, N. Denkov, S. Tcholakova, D. Thorley, S. Stoyanov, Foamability of aqueous solutions: role of surfactant type and concentration, Adv. Colloid Interface Sci. 276 (2020) 102084, https://doi.org/10.1016/j.cis.2019.102084.
[46] B. Petkova, S. Tcholakova, N. Denkov, Foamability of surfactant solutions: Interplay between adsorption and hydrodynamic conditions, Colloids Surf. A Physicochem. Eng. Asp. 626 (2021) 127009, https://doi.org/10.1016/j.colsurfa.2021.127009.
[47] V. Georgiev, Z. Mitrinova, N. Genchev, A. Gers-Barlag, G. Jaunky, N. Denkov, S. Tcholakova, Surface and foam properties of polyvinyl alcohol solutions, Colloids Surf. A Physicochem. Eng. Asp. 681 (2024) 132828, https://doi.org/10.1016/j.colsurfa.2023.132828.
[48] Mitsubishi Chemical Corporation, Physical properties of Sugar Esters, (n.d.). https://www.mfc.co.jp/english/physical.htm (accessed January 12, 2024).
[49] A. Sheludko, Thin liquid films, Adv. Colloid Interface Sci. 1 (1967) 391–464, https://doi.org/10.1016/0001-8686(67)85001-2.
[50] K. Kawahara, C. Tanford, Viscosity and density of aqueous solutions of urea and guanidine hydrochloride, J. Biol. Chem. 241 (1966) 3228–3232.
[51] P.B. Macedo, T.A. Litovitz, On the relative roles of free volume and activation energy in the viscosity of liquids, J. Chem. Phys. 42 (1965) 245–256, https://doi.org/10.1063/1.1695683.
[52] A. Messaâdi, N. Dhouibi, H. Hamda, F.B.M. Belgacem, Y.H. Adbelkader, N. Ouerfelli, A.H. Hamzaoui, A new equation relating the viscosity arrhenius temperature and the activation energy for some newtonian classical solvents, J. Chem. 2015 (2015) e163262, https://doi.org/10.1155/2015/163262.
[53] K.S. Sharma, S.R. Patil, A.K. Rakshit, K. Glenn, M. Doiron, R.M. Palepu, P. A. Hassan, Self-aggregation of a cationic−nonionic surfactant mixture in aqueous media: tensiometric, conductometric, density, light scattering, potentiometric, and fluorometric studies, J. Phys. Chem. B 108 (2004) 12804–12812, https://doi.org/10.1021/jp048294o.
[54] G.B. Dutt, Rotational diffusion of hydrophobic probes in brij-35 micelles: effect of temperature on micellar internal environment, J. Phys. Chem. B 107 (2003) 10546–10551, https://doi.org/10.1021/jp034708m.
[55] M. Tomšič, M. Bešter-Rogač, A. Jamnik, W. Kunz, D. Touraud, A. Bergmann, O. Glatter, Nonionic surfactant brij 35 in water and in various simple alcohols: structural investigations by small-angle x-ray scattering and dynamic light scattering, J. Phys. Chem. B 108 (2004) 7021–7032, https://doi.org/10.1021/jp049941e.
[56] S. Borbély, Aggregate structure in aqueous solutions of Brij-35 nonionic surfactant studied by small-angle neutron scattering, Langmuir 16 (2000) 5540–5545, https://doi.org/10.1021/la991265y.
[57] P.A. Kralchevsky, K.D. Danov, N.D. Denkov, Chemical physics of colloid systems and interfaces, in: K.S. Birdi (Ed.), Handbook of Surface and Colloid Chemistry, 3rd ed., CRC Press, 2008.
[58] B. Sharma, A.K. Rakshit, Thermodynamics of micellization of a nonionic surfactant: Brij 35 in aquo-sucrose solution, J. Colloid Interface Sci. 129 (1989) 139–144, https://doi.org/10.1016/0021-9797(89)90423-2.
[59] M.C. Stumpe, H. Grubmüller, Aqueous urea solutions: structure, energetics, and urea aggregation, J. Phys. Chem. B 111 (2007) 6220–6228, https://doi.org/10.1021/jp066474n.
[60] J.N. Israelachvili, D.J. Mitchell, B.W. Ninham, Theory of self-assembly of hydrocarbon amphiphiles into micelles and bilayers, J. Chem. Soc., Faraday Trans. 2 72 (1976) 1525–1568, https://doi.org/10.1039/F29767201525.
[61] F. Guay, S. Bisaillon, Validation of a mathematical model using the computer for the evaluation of different parameters related to interfaces of air/water and soyabean oil/water systems, J. Colloid Interface Sci. 93 (1983) 25–32, https://doi.org/10.1016/0021-9797(83)90380-6.

[62] S.K. Mishra, D. Panda, Studies on the adsorption of Brij-35 and CTAB at the coal–water interface, J. Colloid Interface Sci. 283 (2005) 294–299, https://doi.org/10.1016/j.jcis.2004.09.017.
[63] B. Lindman, G. Karlström, Nonionic polymers and surfactants: temperature anomalies revisited, Comptes Rendus Chim. 12 (2009) 121–128, https://doi.org/10.1016/j.crci.2008.06.017.
[64] D. Cholakova, Nikolai Denkov, Rotator phases in alkane systems: In bulk, surface layers and micro/nano-confinements, Adv. Colloid Interface Sci. 269 (2019) 7–42, https://doi.org/10.1016/j.cis.2019.04.001.
[65] N.C. Christov, K.D. Danov, P.A. Kralchevsky, K.P. Ananthapadmanabhan, A. Lips, Maximum bubble pressure method: universal surface age and transport mechanisms in surfactant solutions, Langmuir 22 (2006) 7528–7542, https://doi.org/10.1021/la061239h.
[66] K. Golemanov, N.D. Denkov, S. Tcholakova, M. Vethamuthu, A. Lips, Surfactant mixtures for control of bubble surface mobility in foam studies, Langmuir 24 (2008) 9956–9961, https://doi.org/10.1021/la8015386.
[67] K.G. Marinova, N.D. Denkov, Foam destruction by mixed solid-liquid antifoams in solutions of alkyl glucoside: electrostatic interactions and dynamic effects, Langmuir 17 (2001) 2426–2436, https://doi.org/10.1021/la001558n.
[68] K.G. Marinova, R.G. Alargova, N.D. Denkov, O.D. Velev, D.N. Petsev, I.B. Ivanov, R.P. Borwankar, Charging of oil−water interfaces due to spontaneous adsorption of hydroxyl ions, Langmuir 12 (1996) 2045–2051, https://doi.org/10.1021/la950928i.
[69] S. Tcholakova, N.D. Denkov, I.B. Ivanov, Bruce Campbell, Coalescence in β-Lactoglobulin-stabilized emulsions: effects of protein adsorption and drop size, Langmuir 18 (2002) 8960–8971, https://doi.org/10.1021/la0258188.